UNIVERSITI PUTRA MALAYSIA

CHARACTERIZATION OF AMNIOTIC FLUID STEM CELLS (AFSCS)-DERIVED NEURAL STEM CELLS EXOSOMES TREATED WITH ETHANOLIC EXTRACT OF CENTELLA ASIATICA

WAN NUR TIHANI BINTI WAN AHMAD JAILANI

CHARACTERIZATION OF AMNIOTIC FLUID STEM CELLS (AFSCS)-DERIVED NEURAL STEM CELLS EXOSOMES TREATED WITH ETHANOLIC EXTRACT OF *CENTELLA ASIATICA*

WAN NUR TIHANI WAN AHMAD JAILANI

A PROJECT PAPER SUBMITTED AS PARTIAL REQUIREMENT FOR THE DEGREE OF BACHELOR OF SCIENCE (BIOMEDICAL SCIENCES)

DEPARTMENT OF BIOMEDICAL SCIENCES
FACULTY OF MEDICINE AND HEALTH SCIENCES
UNIVERSITI PUTRA MALAYSIA

2022

ABSTRACT

Characterization of Amniotic Fluid Stem Cells (AFSCs)-Derived Neural Stem Cells Exosomes Treated with Ethanolic Extract of *Centella Asiatica*

Wan Nur Tihani Wan Ahmad Jailani[a], Siti Sarah Mustaffa Al-Bakri[a] and Norshariza Nordin[a,b]

[a]Department of Biomedical Sciences and [b]Genetics and Regenerative Medicine (ReGEN) Research Group, Faculty of Medicine and Health Sciences, Universiti Putra Malaysia, Serdang, Malaysia

Introduction: The potential of exosomes as acellular therapy for treating neurodegenerative diseases is emerging. *Centella asiatica* (CA) has been shown to positively mediate production of neurotrophic factors (NF) from stem cells. Previously, we have observed that ethanolic extract of CA (EECA) promoted higher production of NF in the conditioned medium (CM, secretomes) of rat full-term amniotic fluid stem cell line (R3)-derived neural stem cells (NSCs). Therefore, there is a prospect of EECA in enhancing the quality of NSCs-derived exosomes. **Objective:** We aimed to evaluate and characterize the exosomes isolated from the CM of R3-derived NSCs treated with EECA. **Hypothesis:** Treatment of EECA promotes transdifferentiation of R3 into NSCs by generating a higher number and good quality neurospheres, and a higher nestin expression. Next, exosomes with appropriate structures can be isolated from the CM of R3-derived NSCs treated with EECA. **Methodology:** R3 was transdifferentiated into NSCs through a monolayer differentiation assay by culturing 2.6×10^4 R3 cells/cm^2 in Embryoid Body Medium (EBM) with and without treatment for 2 days. This study included four groups: R3 alone (negative control), R3 treated with 1 μg/mL of EECA, 10 μg/mL of EECA, and 50 μM of dBcAMP (positive control). After 2 days, the EBM in all groups was replaced with DMEM/F12 (a resting medium) for 2 days before collecting the CM. On the other hand, the attached NSCs were trypsinized and subjected to form neurospheres confirming the ability of R3 to transdifferentiate into NSCs followed by assessing the quality of neurospheres (size and expression of nestin by immunocytochemistry, ICC). The exosomes were isolated by sequential ultracentrifugation (Beckman Coulter). Later, the structures of the exosomes produced by R3-derived NSCs were observed under JEOL JEM-2100F transmission electron microscopy (TEM) operated at 200 kV, and images were obtained using Gatan Orius software. **Results:** R3-derived NSCs treated with EECA formed a higher number and good quality neurospheres with diameters of 50-100 μm. These neurospheres exhibited a higher expression of nestin. TEM revealed that exosomes of 50–150 nm were successfully isolated from R3-derived NSCs treated with EECA. **Discussion:** The formation of neurospheres and the expression of NSC marker, nestin, confirm the successful transdifferentiation of R3 into NSCs. The treatment of EECA positively influences the quality and quantity of R3-NSCs-derived neurospheres. Based on TEM, EECA-enriched exosomal structures were not compromised upon the treatment with EECA, hence further in-depth investigation is worth pursuing. **Conclusion:** These findings suggest the effect of

EECA as the prospective neuroenhancement adjunct in generating quality exosomes essential for acellular therapy against neurodegenerative diseases.

Keywords: amniotic fluid stem cell, *Centella asiatica*, exosome, neural stem cell, neurodegenerative disease, sequential ultracentrifugation, transmission electron microscopy

ABSTRAK

Pencirian Eksosom Sel Stem Saraf berasal dari Sel Stem Cecair Amniotik (AFSC) yang Dirawat dengan Ekstrak Etanolik *Centella Asiatica*

Wan Nur Tihani Wan Ahmad Jailani[a], Siti Sarah Mustaffa Al-Bakri[a] and Norshariza Nordin[a,b]

[a]Department of Biomedical Sciences and [b]Genetics and Regenerative Medicine (ReGEN) Research Group, Faculty of Medicine and Health Sciences, Universiti Putra Malaysia, Serdang, Malaysia

Pengenalan: Potensi eksosom sebagai terapi aselular untuk merawat penyakit neurodegeneratif semakin muncul. *Centella asiatica* (CA) telah terbukti menjadi pengantara positif dalam penghasilan faktor neurotropik (NF) daripada sel stem. Sebelum ini, kami telah memperhatikan bahawa ekstrak etanolik CA (EECA) menggalakkan pengeluaran NF yang lebih tinggi dalam medium terlazim (CM, secretomes) sel stem cecair amniotik jangka penuh tikus (R3) sel stem saraf (NSC). Oleh itu, terdapat prospek EECA dalam meningkatkan kualiti eksosom yang berasal daripada NSC. **Objektif:** Kami berhasrat untuk menilai dan mencirikan eksosom yang diasingkan daripada CM NSC yang berasal daripada R3 yang dirawat dengan EECA. **Hipotesis**: Rawatan EECA menggalakkan trans pembezaan R3 kepada NSC dengan menjana bilangan neurosfera yang lebih banyak dan berkualiti, dan ekspresi nestin yang lebih tinggi. Seterusnya, eksosom dengan struktur yang sesuai boleh diasingkan dari CM NSC yang berasal dari R3 yang dirawat dengan EECA. **Metodologi:** R3 melalui trans pembezaan kepada NSC melalui kaedah pembezaan ekalapis dengan mengkultur 2.6×10^4 sel R3/cm^2 dalam *Embryoid Body Medium* (EBM) berserta dan tanpa rawatan selama 2 hari. Kajian ini merangkumi empat kumpulan: R3 sahaja (kawalan negatif), R3 dirawat dengan 1 μg/mL EECA, 10 μg/mL EECA, dan 50 μM dBcAMP (kawalan positif). Selepas 2 hari, EBM dalam semua kumpulan digantikan dengan DMEM/F12 (medium rehat) selama 2 hari sebelum pengumpulan CM. Di samping itu, NSC yang terlampir telah ditanggalkan dengan kaedah tripsin, kemudian dibentuk menjadi neurosfera bagi mengesahkan keupayaan R3 untuk melalui trans pembezaan kepada NSC diikuti dengan penilaian kualiti neurosfera (saiz dan ekspresi nestin oleh imunositokimia, ICC). Eksosom diasingkan oleh pengultraemparan berurutan (Beckman Coulter). Kemudian, struktur eksosom yang dihasilkan oleh NSC yang berasal dari R3 diperhatikan menggunakan mikroskop elektron penghantaran JEOL JEM-2100F (TEM) yang dikendalikan pada 200 kV, dan imej diperolehi menggunakan perisian Gatan Orius. **Hasil dapatan:** NSC yang berasal dari R3 yang dirawat dengan EECA membentuk bilangan neurosfera yang lebih banyak dan berkualiti tinggi dengan diameter 50-100 μm. Neurosfera ini mempamerkan ekspresi nestin yang lebih tinggi. TEM menunjukkan bahawa eksosom bersaiz 50-150 nm berjaya diasingkan daripada NSC yang berasal dari R3 yang dirawat dengan EECA. **Perbincangan:** Pembentukan neurosfera dan ekspresi penanda NSC, nestin, mengesahkan kejayaan trans pembezaan R3 kepada NSC. Rawatan EECA mempengaruhi secara positif kualiti dan kuantiti neurosfera yang berasal dari R3-NSCs. Berdasarkan TEM, struktur eksosom yang diperkayai EECA tidak terjejas, oleh itu kajian susulan wajar diambil. **Kesimpulan:** Penemuan ini mencadangkan kesan

penggalakan (*neuroenhancement)* EECA yang dijangka berpotensi menghasilkan eksosom berkualiti dalam terapi aselular bagi penyakit neurodegeneratif.

Kata kunci: sel stem cecair amniotik, *Centella asiatica*, eksosom, sel stem saraf, penyakit neurodegeneratif, pengultraemparan berurutan, mikroskop elektron penghantaran

ACKNOWLEDGEMENTS

In the name of Allah, the Most Gracious and Merciful.

I wish to express my special appreciation to my loving parents, Wan Ahmad Jailani Wan Mahmud and Wan Nor Haryati Wan Zain; and also to my supportive brothers.

My sincere gratitude goes to Assoc. Prof. Dr. Norshariza Nordin for her excellent guidance and advice in accomplishing this research.

I am also indebted to my wonderful mentor, Siti Sarah Mustaffa Al Bakri. Praise be to Allah, I have accomplished my FYP thanks to the help from Khairul Akmal, laboratory staff, my friends, and everyone involved.

TABLE OF CONTENT

LIST OF TABLES

LIST OF FIGURES

LIST OF ABBREVIATIONS

mL	microliter
nm	nanometer
β	beta
µg	microgram
µL	microliter
µm	micrometer
µM	micromolar
AD	Alzheimer's Disease
AF	amniotic fluid
AFSCs	amniotic fluid stem cells
Aβ	amyloid-β
BAR	Bin, Amphiphysin, Rvs
BDNF	brain-derived NF
bFGF	Basic Fibroblast Growth Factor
BSC	biosafety cabinet
CA	*Centella asiatica*
CD117	type III receptor tyrosine kinase for stem cell factor
CM	conditioned medium
CNS	central nervous system
CTCF	corrected total cell fluorescence
DAPI	4',6-diamidino-2-phenylindole
dBcAMP	dibutyryl-cAMP
DIV	day in vitro
DM SO	dimethyl sulfoxide
DMEM	Dulbecco's Modified Eagle Medium
EBM	Embryoid Body Medium
EDTA	ethylenediaminetetraacetic acid
EECA	ethanolic extract of CA
EGF	Epidermal Growth Factor
EM	electron microscopy
ESCs	embryonic stem cells
ESE	early-sorting endosome
ESM	embryonic stem cells medium
FBS	fetal bovine serum
GABA	gamma-aminobutyric acid
GMEM	Glasgow Minimum Essential Medium
GCL	granule cell layer
HB	*Hydrocotyle bonariensis*
HPLC	high-performance liquid chromatography
hPSCs	human pluripotent stem cells
HS	*Hydrocotyle sibthorpioides*
ICC	immunocytochemistry

ILV	intraluminal vesicles
iPSCs	induced pluripotent stem cells
kV	kilovolt
LIF	leukemia inhibitory factor
LSE	late-sorting endosomes
ML	molecular layer
MVB	multivesicular bodies
ND	neurodegenerative diseases
NF	neurotrophic factor
NGF	nerve growth factor
NSCs	neural stem cells
NTA	nanoparticle tracking analysis
PBS	phosphate buffer solution
R3	rat full-term amniotic fluid stem cells
RNA	ribonucleic acid
rpm	revolutions per minute
SD	standard deviation
SEM	scanning EM
SGZ	subgranular zone
SVZ	subventricular zone
TEM	transmission electron microscopy
TPC	total phenolic content
V	ventricular space
VZ	ventricular zone

CHAPTER 1

INTRODUCTION

1.1 Background

Neurodegenerative diseases (ND) pose debilitating health threats to human due to irreversible functional damage as well as insufficient regeneration process of the nervous system (Ford et al., 2020). ND include Parkinson's disease, stroke, epilepsy, multiple sclerosis, spinal cord injury and neuropathic pain. Undergoing research are being actively encouraged to unravel therapeutic actions against neurodegeneration.

Therapies for ND encompass several strategies involving stem cells, known as stem cell-based therapy. Cellular therapy is achieved through stem cell transplantation to replace damaged tissue, and regeneration of the damaged or lost neuron. For example, neural stem cells (NCSs) transplantation can be done to treat stroke (De Gioia et al., 2020). Due to the invasiveness of procuring NSCs from the brain, it would be ideal to have a safer source of NSCs. Amniotic fluid stem cells (AFSCs) can be collected in full-term pregnancies as medical waste or non-brain source (Mun-Fun et al., 2015). The neurogenic potential of AFSCs as demonstrated by De Coppi et al. (2007) makes these broadly multipotent stem cells a possible attractive source of NSCs for use in therapy.

However, the challenges of the treatments using stem cells are being pointed out regarding the safety, feasibility and efficiency. Transplantation of stem cells may not be effective as cells may not successfully integrate and fail to survive in vivo

(Thored et al., 2006). Therefore, designation of more appropriate strategies to treat ND is in demand.

It has been discovered that secretomes, or conditioned medium (CM) of stem cells have great involvement in mediating intercellular communication via the paracrine effect (Arrigo et al., 2019). Exosomes, the nano-sized component of the secretomes, have potential in inhibiting neuronal death via the therapeutic effects of neurotrophic factor (NF; Huang et al., 2014). Exosomes are therefore gaining continuous interest as a good option for treatments against ND (Kalluri & LeBleu, 2020). This approach is known as acellular therapy. The limitations of cellular therapy can be potentially overcome by using stem cells-derived exosomes in terms of safety and effectiveness due to its lower risk of immunogenicity and tumorigenicity (De Gioia et al., 2020; Maguire, 2014; Seyfizadeh et al., 2019). Besides, exosomes have the ability to cross the blood-brain barrier, can be subjected to precise dosing and are devoid of risk of immunocompatibility. The non-invasive administration of exosomes such as via intranasal route also renders acellular therapy a better approach over cellular therapy (Long et al., 2017).

In searching for alternative treatments for ND, neuroregenerative properties of natural products like *Centella asiatica* (CA) have also been brought into the spotlight. Through neuroprotection effect, CA is presumed to be helpful in treating ND as it can protect nerve cells from death (Yogeswaran et al., 2016). The role of CA in offering a wide range of therapeutic values is proposed to be an ideal neuroenhancement adjunct in the production of good quality exosomes. Thus, the present study is interested in

assessing the effect of ethanolic extract of CA (EECA) on exosomes produced by AFSCs-derived NSCs.

1.2 Problem Statement

The study of the alternative treatments for ND is an emerging research direction. As the potential of exosomes as acellular therapy for treating ND gains accumulating attention, the research of good sources of exosomes is at its preliminary stage. It is crucial to choose the ideal stem cell type that can generate good quality exosomes to elucidate their therapeutic potential. On this basis, there is a need to emphasize the proof of concept that AFSCs can be one of the best sources of exosomes that can carry therapeutic values against ND. This study aims to explore the effect of CA on exosomes generated from rat full-term amniotic fluid stem cell line (R3)-derived NSCs. This demands characterization of the exosomes generated from the R3-derived NSCs for future therapeutic applications.

1.3 Hypothesis

It is hypothesized that the treatment of EECA promotes transdifferentiation of R3 into NSCs by generating a higher number and good quality of neurospheres and higher nestin expression. The EECA treatment does not compromise the structure of the exosomes isolated from the CM of R3-derived NSCs.

1.4 Objectives

General objective: To assess the effect of ethanolic extract of *Centella asiatica* (EECA) on exosomes produced by rat full-term amniotic fluid stem cells (R3)-derived neural stem cells (NSCs).

Specific objectives:

1. To examine the effect of EECA on the quality and quantity of R3-NSCs-derived neurospheres.
2. To confirm the presence of R3-derived NSCs in neurospheres via the expression of the NSC marker, nestin, by immunocytochemistry.
3. To characterize EECA-enriched exosomes after isolation with sequential ultracentrifugation technique using transmission electron microscopy (TEM).

CHAPTER 2

LITERATURE REVIEW

2.1 Neurodegenerative diseases (ND)

2.1.1 Background of neurodegenerative diseases (ND)

Neurodegenerative diseases (ND) affect millions of individuals worldwide; it is an umbrella term to describe conditions in which nerve cells in the nervous system progressively lose function followed by death, characterized by irreversible functional damage as well as insufficient regeneration process of the adult nervous system (Ford et al., 2020; National Institute of Environmental Health Sciences, retrieved January 23, 2022).

ND include Parkinson's disease, stroke, epilepsy, multiple sclerosis, spinal cord injury and neuropathic pain. Patients suffering from Parkinson's disease face symptoms like bradykinesia, cognitive incompetency, and tremor due to the progressive loss of dopaminergic neurons in the substantia nigra. Available treatments include levodopa administration to alleviate patients' conditions; however, this treatment is not profound enough to aid the production of dopamine as the progression of the disease becomes severe (Figge et al., 2016; Poewe, 2009). Stroke, on the other hand, is a condition where the blood flow in a part of a patient's brain is suddenly interrupted, leading to the death of heterogeneity of neuronal cell types (Ford et al., 2020). Learning and memory disorders/dementia, known as Alzheimer's Disease (AD) can severely affect the cognitive processes related to the hippocampus that are crucial in learning and memory. These are caused by degeneration of cholinergic neurons and

synapses- or presence of extracellular amyloid-β (Aβ) plaques and intracellular neurofibrillary tangles which are neurotoxic. Unfortunately, this condition is untreatable but can be potentially improved with regenerative medicine.

2.1.2 Conventional treatments for neurodegenerative diseases (ND)

Limitations arise as the human body cannot replace the damaged or dead neurons to overcome ND (JPND, retrieved January 23, 2022). Regeneration is making a significant advancement in clinical practice with the aim of restoring disease and damaged tissues or organs to counterbalance the maladies caused by neurodegeneration (Ford et al., 2020; Mao & Mooney, 2015). Therein, a number of methods have been designed to promote neuroregeneration in the nervous system. Therapies for ND encompass several strategies involving stem cells, known as stem cell-based therapy.

Cellular therapy is done through stem cell transplantation, whereby stem cells replace damaged tissue and also through regeneration of damaged or lost neurons (Seyfizadeh et al., 2019). Transplantation of stem cells aims to reduce neuroinflammation besides promoting neuronal plasticity and replacement of cells (De Gioia et al., 2020). Speaking of regeneration, regenerative medicine is becoming a field with burgeoning importance which combines engineering and science disciplines to restore diseases and injured tissues or organs caused by age, trauma, or congenital defects (Mao & Mooney, 2015). In contrast with the transplantation of intact organs, regenerative medicine may overcome the limitations of shortage of donor supply and detrimental immune complications (Bajaj et al., 2014).

Human pluripotent stem cells (hPSCs)-based therapies can lead to neural tissue regeneration in stroke conditions by neuronal replacement, neuroprotection, modulation of inflammation, and angiogenesis (Ford et al., 2020). Preclinical studies using stem cells have also been made using animal models in the attempt to replace the loss of neurons in AD, such as via therapies using hPSCs which have recorded positive outcomes in learning and memory.

2.1.3 Challenges in treating neurodegenerative diseases (ND)

However, the challenges of the treatments using stem cells are being pointed out regarding the safety, feasibility and efficiency. As the success of the cell implants is afflicted by crucial factors like cell survival and cell-conditioned culture medium, it is important to acknowledge the relevance of using this cellular therapy approach in treating ND (Bi et al., 2007, as cited in Seyfizadeh et al., 2019). Major safety risks posed by stem cells include inflammation, teratoma formation, undesired cell differentiation, and immune rejection (De Gioia et al., 2020). Genetic stability of stem cells such as induced pluripotent stem cells (iPSCs) is another concern as it can give rise to tumors. Mandai et al. (2017) detected mutation which may be suggestive of tumorigenicity in iPSCs. Studies also reported the limitations of using mesenchymal stem cells in regenerative medicine since the method of infusion, standardized ex vivo expansion protocol, effective route of delivery, dosage infusion, and frequency of administration of the stem cells are not clearly defined (Kandoi et al., 2018; Zaher et al., 2014).

Transplantation of stem cells may not be effective as cells may not successfully integrate and fail to survive in vivo (Thored et al., 2006). In particular, using NSCs obtained from humans to treat ND still requires extensive research to ascertain optimal

cell source and safety in the long run before it can be translated into clinical practice. Tissue engineering and regenerative medicine have emerged as an industry. In essence, the use of stem cells in regenerative medicine necessitates tight regulations on the cells intended for the therapeutic effects to ensure safety and efficacy post-transplantation (Mao & Mooney, 2015).

For therapeutic interventions that target the brain, the blood-brain barrier, a microvasculature structure composed of capillaries that protect the central nervous system (CNS) from harmful substances, poses a hurdle in inducing brain repair mechanisms as it limits the entry of stem cells (Gonzales-Portillo et al., 2014). Apart from that, the invasive administration of stem cells such as via intracerebroventricular injection as illustrated in Figure 2.1 and ethical issues of destroying embryos in generating embryonic stem cells (ESCs) pose challenges.

Altogether, the aforementioned limitations make it necessary to review the current approaches to design more appropriate strategies to treat ND.

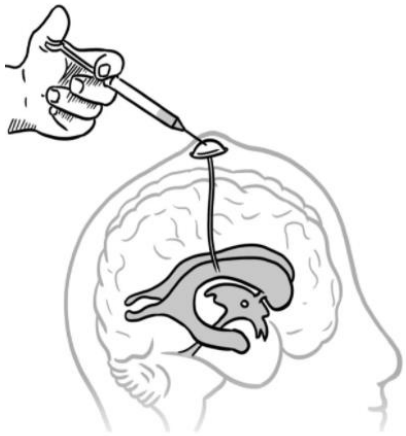

Figure 2.1: Intracerebroventricular injection of stem cells. The administration of stem cells by this method is invasive. Adapted from Kim et al. (2021).

2.2 Stem cells

2.2.1 Definition and types of stem cells

Stem cells are building blocks of tissue and organ in an organism which are undifferentiated and have the ability to give rise to differentiated cells. There exist different potency levels, defined as the ability to differentiate into different cell types; including totipotent, pluripotent, multipotent, oligopotent and unipotent (Figure 2.2). Stem cells can be categorized based on their potency (Kolios & Moodley, 2012). Totipotent stem cells generate embryonic and extraembryonic tissue. Pluripotent stem cells can differentiate into tissue from mesoderm, endoderm or ectoderm, except the placenta. Example of pluripotent stem cells are ESCs and somatic cells that undergo reprogramming known as iPSCs. Meanwhile, multipotent stem cells such as mesenchymal stem cells and NSCs may differentiate into different products such as bone, cartilage, adipose tissue and neural cells from a single germ layer. Oligopotent and unipotent stem cells have limited differentiation abilities as they can only differentiate into several lineages of a specific tissue, and one specific type of cell, respectively.

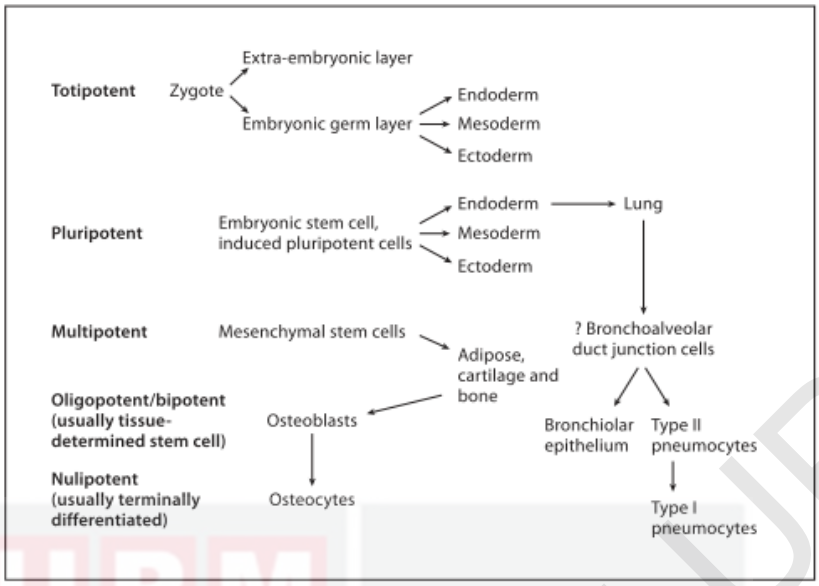

Figure 2.2: Stem cells potency. Totipotent stem cells generate embryonic and extraembryonic tissue. Pluripotent stem cells can differentiate into tissue from mesoderm, endoderm or ectoderm while multipotent cells differentiate into multiple products such as bone, cartilage and adipose tissue from a single germ layer. Oligopotent and unipotent stem cells have limited differentiation abilities. Adapted from Kolios & Moodley (2012).

2.2.2 Characteristics of stem cells

Stem cells pose unique characteristics that set them apart from somatic cells which are self-renewal and potency (Kolios & Moodley, 2012). Self-renewal characterizes the ability of stem cells to divide extensively, while potency characterizes the ability to differentiate into distinct types of cells (Figure 2.3).

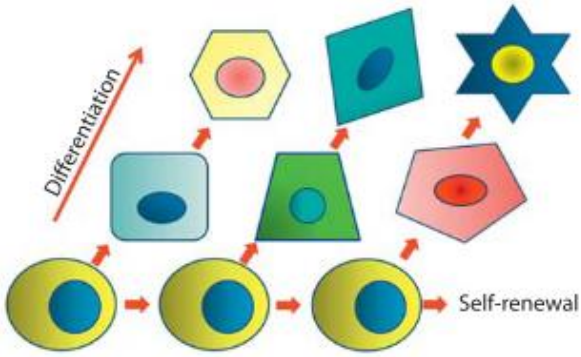

Figure 2.3: Differentiation and self-renewal in stem cells. Stem cells extensively divide through self-renewal and undergo differentiation into distinct types of cells. Adapted from Kolios & Moodley (2012).

2.2.3 Therapeutic potential of stem cells

Stem cells serve as the body's internal repair system. As long as an organism is alive, stem cells may indefinitely replenish and generate new cells (Ota, 2008). Stem cells' fate is determined by the organ in which they are found. In general, the therapeutic potential of stem cells to treat diseases can be divided into cellular and acellular therapy.

In cellular therapy, stem cells are incorporated for the replacement and regeneration of damaged cells or organs such as through stem cell transplantation. On the other hand, stem cells make it possible to explore the pathology and progress of a disease. Cell lines particular to a disease can be produced and employed in medication research (Kolios & Moodley, 2012).

On the contrary, acellular therapy is a type of method that does not use stem cells. It has been discovered that secretomes, or CM of stem cells have great involvement in mediating intercellular communication via the paracrine effect (Arrigo

et al., 2019). Exosomes, as the smallest component of the secretomes are gaining continuous interest as a good option for treatments for ND (Kalluri & LeBleu, 2020).

2.2.4 Transdifferentiation of stem cells

Among the methods that may compensate the damaged nerve cells in neurodegeneration is by transforming certain stem cells type into stem cells of the nervous system. Theoretically, many types of stem cells can be induced into NSCs intended for ND therapy including mesenchymal stem cells (Casarosa et al., 2014). It has been shown that NSCs can also be derived from AFSCs in vitro (Pozzobon et al., 2010). This process is known as transdifferentiation, which is an induced conversion of a stem cell type to another without the involvement of pluripotent state.

2.2.5 Amniotic fluid stem cells (AFSCs)

AFSCs are obtained from amniotic fluid (AF) during amniocentesis whereby the number and properties of cells are influenced by gestational age and fetal pathological factors (Walentowicz et al., 2022). Other than amniocentesis in mid-term pregnancies or second trimester (18-24 weeks of gestation), AFSCs can also be collected in full-term pregnancies or third trimester (38-40 weeks of gestation) as a medical waste through a non-invasive procedure (Mun-Fun et al., 2015).

In comparison of the two methods, full-term AF is more favored for the isolation of AFSCs than mid-term AF since it is easier to procure through normal deliveries that is artificial rupture membrane or cesarean section deliveries (Hamid et al., 2017). More importantly, full-term AF is subjected to minimal ethical concern and potential risks to the mother and the baby (Hamid et al., 2017). AFSCs do not form tumors upon transplantation, hence are regarded to be safe (Pozzobon et al., 2010).

AFSCs are capable of giving rise to adipogenic, osteogenic, myogenic, endothelial, neurogenic, and hepatogenic lineages, ectoderm, mesoderm, and endoderm germ layers (De Coppi et al., 2007).

Rat full-term amniotic fluid stem cells (R3) are an in-house established cell line by Mun Fun and colleagues (2015). This group of researchers has successfully established primary cells designated as R3 from the AF of a rat model through magnetic activated cell sorting to select c-kit (CD117, type III receptor tyrosine kinase for stem cell factor) positive cells. R3 differentiation capacity falls between pluripotent and multipotent types of stem cells, specifically broadly multipotent. The population doubling time of R3 was recorded to be around 38.60 ± 3.52 h. Oct4; a transcription factor involved in pluripotent stem cells maintenance, Nanog; a transcription factor involved in pluripotency regulation, stage-specific embryonic antigen-1; an embryonic stem cells surface marker, and Sox2; a pluripotency marker, were all expressed in R3.

2.2.6 Neural stem cells (NSCs)

NSCs are located in the subventricular zone (SVZ) and subgranular zone (SGZ) as illustrated in Figure 2.4, where neurogenesis takes place (Ding et al., 2020; Grochowski & Maciejewski, 2018). The ventricular area and SVZ are separated by the ependymal cell layer. Neurogenesis is a vital process of regenerating new and functional neurons in NSCs (Y. Li, 2020). The NSCs located in the SVZ are known as type B cells; they generate type C cells (actively dividing intermediate cells) that further produce type A cells (neuroblasts; Casarosa et al., 2014). GABAergic granule neurons are later produced from neuroblasts upon migration away from the SVZ. In the dentate gyrus of the hippocampus of adult mammalian brains, type I progenitors (astrocyte-like NSCs) within the SGZ may divide to produce type II cells (immature

proliferating progenitors; Casarosa et al., 2014). Consequently, type II cells form migrating neuroblasts and develop into functional granule neurons in the dentate gyrus.

The integrative process of NSCs is crucial to contribute to a functional integrity of the adult brain which is closely related to neurological wellness. Newborn neurons created from NSCs in adult neurogenic niches are essential for brain homeostasis responsible for information processing, cognitive functions, and affective responses (Goncalves et al., 2016). NSCs can be procured from neural tissue, derived from pluripotent stem cells either through the formation of embryoid bodies or three-dimensional aggregates, or genetically manipulated and differentiated in vitro (Casarosa et al., 2014).

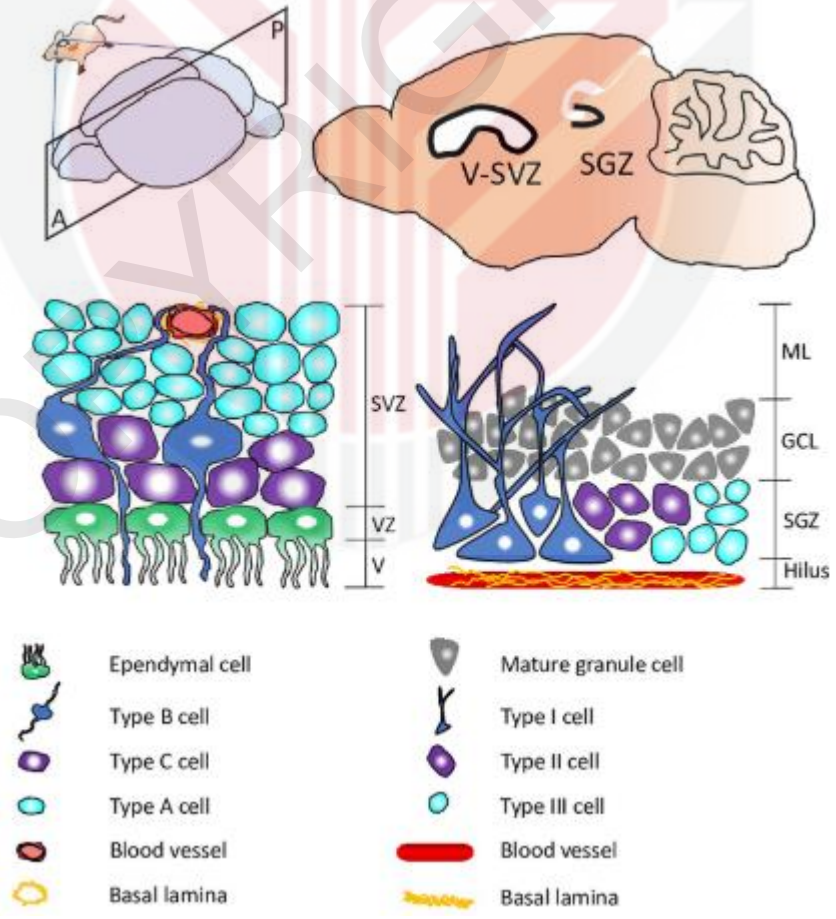

Figure 2.4: NSCs located in the subventricular zone (SVZ) and the subgranular zone (SGZ) of mammalian brain. Type B NSCs are located in the SVZ while type I

are in the SGZ. GCL, granule cell layer; ML, molecular layer; V, ventricular space; VZ, ventricular zone. Adapted from Ding et al. (2020).

Characteristics of NSCs include self-renewal, neural tripotency (the capability to differentiate into neurons, astrocytes and oligodendrocytes) and the ability for in vivo regeneration post-transplantation (Casarosa et al., 2014).

To characterize neural stem cells, immunocytochemistry (ICC) analysis can be performed to detect the expression of molecular markers (Merck, retrieved April 25, 2022). Among them are nestin, Sox2, and Musashi, where these markers' expression characterizes NSCs. In contrast, highly differentiated lineage markers such as βIII-tubulin for neurons are not significantly expressed in NSCs. Assessment of NSCs can also be done through neurospheres' formation and observation by neurosphere assay in vitro as illustrated in Figure 2.5a (Soares et al., 2021). Neurospheres consist of neural progenitor cells deriving from a single NSC. In this technique, NSCs are grown in spherical aggregates, and demonstration of NSCs markers can be further carried out by ICC. The expression of markers like nestin ascertains that cells are NSCs (Figure 2.5b).

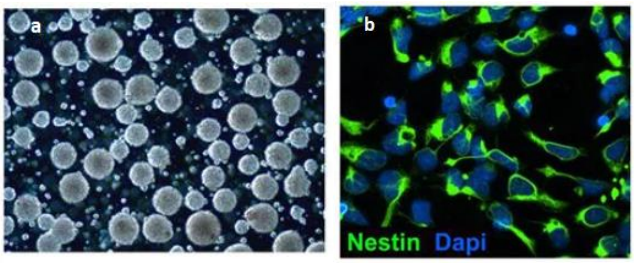

Figure 2.5: NSCs (a) forming floating neurospheres and (b) expressing nestin marker. Neurospheres are grown in spherical aggregates. NSCs express nestin in

green and the nuclei are counterstained in blue. Adapted from Merck (retrieved April 25, 2022).

2.2.6.1 Therapeutic potential of neural stem cells (NSCs)

With the discovery of NSCs, the progression of ND inclusive of non-treatable ones can be hampered (Ota, 2008). In stem cell transplantation, NSCs are differentiated into neurons to achieve reintegration in ND. For example, Zheng and colleagues recorded improvement in motor functions upon administration of NSCs in the ipsilateral striatum region of animal models with stroke (De Gioia et al., 2020). Growing evidence also highlighted the use of NSCs derived from fetal- and adult CNS in clinical applications (Casarosa et al., 2014). Although some of the studies have successfully isolated NSCs from rodents' and humans' brains at different developmental stages, harvesting these cells from their natural niches and the expansion in vitro are challenging due to the requirement of optimum physiological conditions.

Interestingly, De Gioia and colleagues (2020) reviewed the use of stem cells' secretomes as an alternative to using stem cells directly for neurodegenerative therapies. The study showed that the administration of secretomes successfully ameliorated Parkinson's disease in terms of motor functions and enhanced substantia nigra and striatal neurons in the 6-hydroxydopamine rat model. This observation was even more pronounced than those transplanted with stem cells.

In line with the search for therapeutic interventions against ND, the scientific community has brought secretomes into the spotlight as a better approach than cellular therapy. Thereby, the relevance of using non-brain sources to eliminate the invasive

procedures of isolating NSCs, such as by transdifferentiating AFSCs into NSCs in vitro for an easier and safer option is surfacing.

2.3 Exosomes

2.3.1 Definition of exosomes

Stem cells secrete soluble components and extracellular vesicles in the secretomes (Figure 2.6). Secretomes contain therapeutic effects including antifibrotic, antiapoptotic, anti-inflammatory, and immune-modulatory properties (Timmers et al., 2008; Tögel et al., 2005; Sears & Ghosh, 2011). The burgeoning roles of secretomes are extensively studied and discovered to be responsible for the mediation of intercellular communication via paracrine effect. Mushahary and colleagues (2017) categorize extracellular vesicles by size, namely- exosomes (30-150 nm), microvesicles (100-1000 nm) and apoptotic bodies (1000-3000 nm). Exosomes having the smallest size among all components are believed to be a good candidate for ND therapy due to exosomes' ability to cross the blood-brain barrier unlike stem cells (Seyfizadeh et al., 2019). Exosomes are released by any type of cell in normal and diseased conditions to transport cargo such as nucleic acids, proteins, lipids and metabolites (Kalluri & LeBleu, 2020; Khatun et al., 2016). The delivery of exosomes for therapeutic uses can be done intranasally. For example, Long et al. (2017) demonstrated that exosome's intranasal administration reduced neuron loss and inflammation. A good source of exosomes for ND therapy is the CM of NSCs.

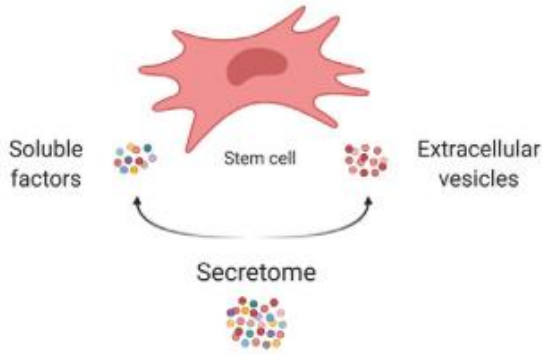

Figure 2.6: Secretion of soluble factors and extracellular vesicles by stem cells. Soluble components and extracellular vesicles are released in the secretomes or conditioned medium (CM). Adapted from Daneshmandi et al. (2020).

Biogenesis of exosomes begins with endocytosis and plasma membrane invagination of extracellular components and fluid as illustrated in Figure 2.7. Later, the budding process results in generation of early-sorting endosome (ESE). Maturation of ESEs gives rise to late-sorting endosomes (LSEs). Invagination of plasma membrane then leads to formation of multivesicular bodies (MVBs). MVBs are composed of intraluminal vesicles (ILVs), which become exosomes in the upcoming stage. There are multiple fates of MVBs, they may be degraded upon fusion with lysosomes or autophagosomes. If fusion of MVBs occurs with the plasma membrane, MVBs will be released via exocytosis as exosomes.

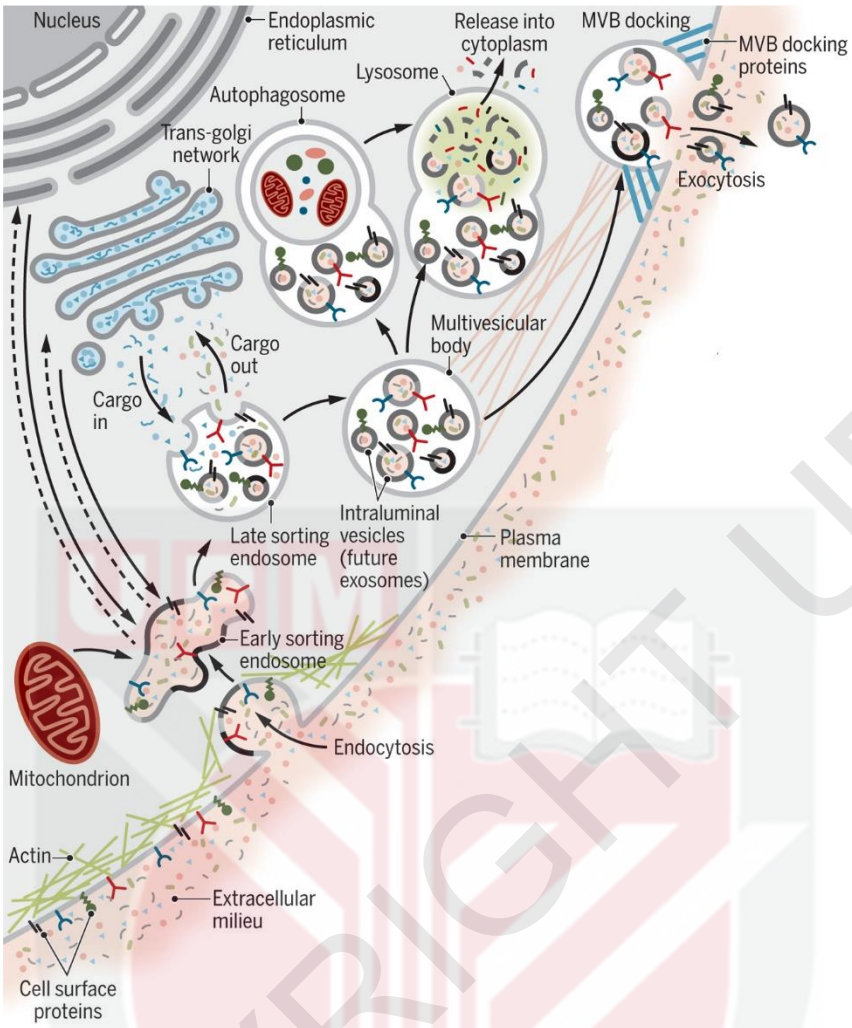

Figure 2.7: Biogenesis of exosomes. Budding process forms early-sorting endosome (ESE) which later matures into late-sorting endosomes (LSEs). Multivesicular bodies (MVBs) which are later formed from invagination of the plasma membrane are composed of intraluminal vesicles (ILVs). MVBs may be degraded or released as exosomes. Adapted from Kalluri and LeBleu (2020).

2.3.2 Isolation of exosomes

Various approaches are used to isolate exosomes from other components in CM. These include ultracentrifugation-based, size-based, exosome precipitation, immunoaffinity capture-based, and microfluidics-based methods (P. Li et al., 2017). Recently, many commercial kits have been developed to isolate exosomes such as exoEasy Maxi kit (QIAGEN), MagCapture™ Exosome Isolation Kit PS (Wako) and Minute™ Hi-Efficiency Exosome Precipitation Reagent (Invent). Although these

commercial kits are advantageous due to time-saving, the exosomal yield and purity are not high (Zhang et al., 2020).

2.3.2.1 Principles of isolation of exosomes

Centrifugation separates a heterogeneous mixture into components according to their density, size and shape by centrifugal force (P. Li et al., 2017). Particles with smaller size and density sediment later than the bigger ones. Centrifugation at very high centrifugal forces is known as ultracentrifugation, with centrifugal force in the range of 100,000-120,000 x g. The ultracentrifugation technique is a gold standard for isolating exosomes and is preferred among researchers for its minimal skills requirement, long-term use of an ultracentrifuge, and large-scale sample processing.

2.3.2.2 Principles of sequential ultracentrifugation

Sequential ultracentrifugation allows isolation of exosomes based on size and density by a series of centrifugation at different centrifugal forces and durations (P. Li et al., 2017). In this approach, lower speed centrifugation eliminates dead cells and cell debris, while higher speed is meant for separation of exosomes.

2.3.3 Morphological characterization of exosomes

From the size to morphology, ribonucleic acid (RNA) content, surface protein markers; diverse characteristics of exosomes are extensively studied (Cross, Linker & Leslie, 2016; Khatun et al., 2016). In the morphological characterization of exosomes, electron microscopy (EM) is typically used. Observation of exosomes is otherwise undetectable by optical microscopes. The analysis of exosomes isolated from NSCs reflects the quality of exosomes, thus considered fundamental prior to establishing therapy using exosomes in patients suffering from ND.

2.3.3.1 Principles of scanning electron microscopy (SEM) and transmission electron microscopy (TEM)

There are two types of EM utilizing high-energy electron beams, namely scanning EM (SEM) and TEM. SEM enables visualization of a sample's surface structure while TEM allows for observation of detailed internal structure in addition to the particle size distribution (Zhang et al., 2020). TEM has a higher magnification at 1,000,000x than SEM at 100,000x (Reza et al., 2020). The resolution of TEM (0.07 nm) is also higher than SEM (2-10 nm). In SEM, an accelerated beam of electron from electron gun passes through condenser and objective lenses, resulting in the generation of signals at the sample's surface. On the other hand, TEM applies transmission of electron beam through a sample. The electron beam passes through condenser lenses prior to magnification by objective lenses to produce a final image of the sample.

2.3.3.2 Advantages/disadvantages of scanning electron microscopy (SEM) and transmission electron microscopy (TEM)

While both types of microscopes can assess the morphology of exosomes, the images produced are slightly different in which exosomes appear as round spheroids under SEM but show central depression as an attribute of artifact in TEM analysis. Both methods exhibit similar size as recorded by Cross, Linker and Leslie (2016) in terms of diameters. TEM is preferred in cases where large-scale analysis need to be done rapidly (Zhang et al., 2020).

2.3.4 Therapeutic potentials of exosomes

The activity of extracellular vesicles released by stem cells is claimed to encourage disease amelioration by means of cellular communication and involvement in disease progression rather than through direct cell replacement (Mushahary et al.,

2017). In the same manner, administration of paracrine factors derived from NSCs is implied to achieve therapeutic benefits against ND (Vogel et al., 2018).

Ultimately, the limitations of cellular therapy can be potentially overcome by therapy using stem cells-derived exosomes in terms of safety and effectiveness due to its lower risk of immunogenicity and tumorigenicity (De Gioia et al., 2020; Maguire, 2014; Seyfizadeh et al., 2019). Besides, exosomes have the ability to cross blood-brain barrier, can be subjected to precise dosing and are devoid of risk of immunocompatibility

Accumulating evidence suggests the therapeutic use of exosomes, one of the pillars in acellular therapy. Therapeutic outcomes may be produced as exosomes carry NF. Boyd and Gordon (2003) noted that NF can enhance motor neuron regeneration (as cited in Jonsson et al., 2013). Brain-derived NF (BDNF) which is expressed in brain regulates neuronal survival and development (Chung et al., 2020). BDNF exerts neuroprotective effect and can inhibit apoptosis in ND, hence playing a significant role in overcoming degeneration (Huang et al., 2014). Nerve growth factor (NGF) is also essential for development of neurons. Exosome derived from NSCs holds significant potential as an alternative for conventional treatments for ND. Having this in mind, scientists seek to utilize acellular therapy to target specific neurons responsible for neurodegeneration problems such as in Parkinson's disease, Huntington's disease and amyotrophic lateral sclerosis.

2.3.5 Role of natural products to enhance quality of exosomes

As a country rich in diversity of natural products, herbal extracts are widely studied for their medical benefits. Therefore, it is beneficial to have a natural product

that can have positive influence in treating ND. The key mechanism may lie in the potential of the herbal extract to enhance the quality of exosomes. For example, neuroregenerative properties of the natural product can be of significant influence in achieving reparative actions in diseases caused by neurodegeneration.

2.4 *Centella asiatica*

2.4.1 Definition of Centella asiatica

In the search for alternative interventions against ND, natural products or herbs that can naturally provide therapeutic properties are brought into research. One of the scientifically studied herbs is *Centella asiatica* (CA) as shown in Figure 2.8. CA or asiatic pennywort is commonly known as *pegaga* in Malaysia (Maulidiani et al., 2014). Geographically, it is found throughout the majority of tropical and subtropical countries in swampy and damp regions of fields (Gohil et al., 2010). Among them are Southeast Asia, South Africa and Eastern Europe. This herb has been known for generations as a culinary vegetable; it is occasionally consumed raw as a salad (Hashim et al., 2011). Apart from its local usage, CA also has essential roles in other parts of the world such as in traditional Chinese and Ayurvedic medicinal practitioners due to its link with cognitive benefits (Matthews et al., 2019). Other varieties of *pegaga* are *Hydrocotyle bonariensis* (HB) or large leaf marsh pennywort; and *Hydrocotyle sibthorpioides* (HS) or lawn marsh pennywort (Maulidiani et al., 2014).

Figure 2.8: *Centella asiatica*. The leaves are fan-shaped and green in color. Image credited to Winterton (2018).

2.4.2 Properties of Centella asiatica

CA, a triterpene-rich medicinal herb, is highly associated with therapeutic benefits (Nadia et al., 2019). Triterpenes, also called saponins, include asiatic acid, asiaticoside, madecassic acid, and madecassoside (Hashim et al., 2011). Other than that, CA contains phenolics (chlorogenic acids), flavonols (quercetin and kaempferol), and polyacetylene (Govindan et al., 2007; Maulidiani et al., 2014). Analysis of types of triterpenes by high-performance liquid chromatography (HPLC) as illustrated in Figure 2.9 shows the following quantification: madecassoside (3.70%), asiaticoside (3.57%), madecassic acid (1.91%) and asiatic acid (1.73%; Hafiz et al., 2020).

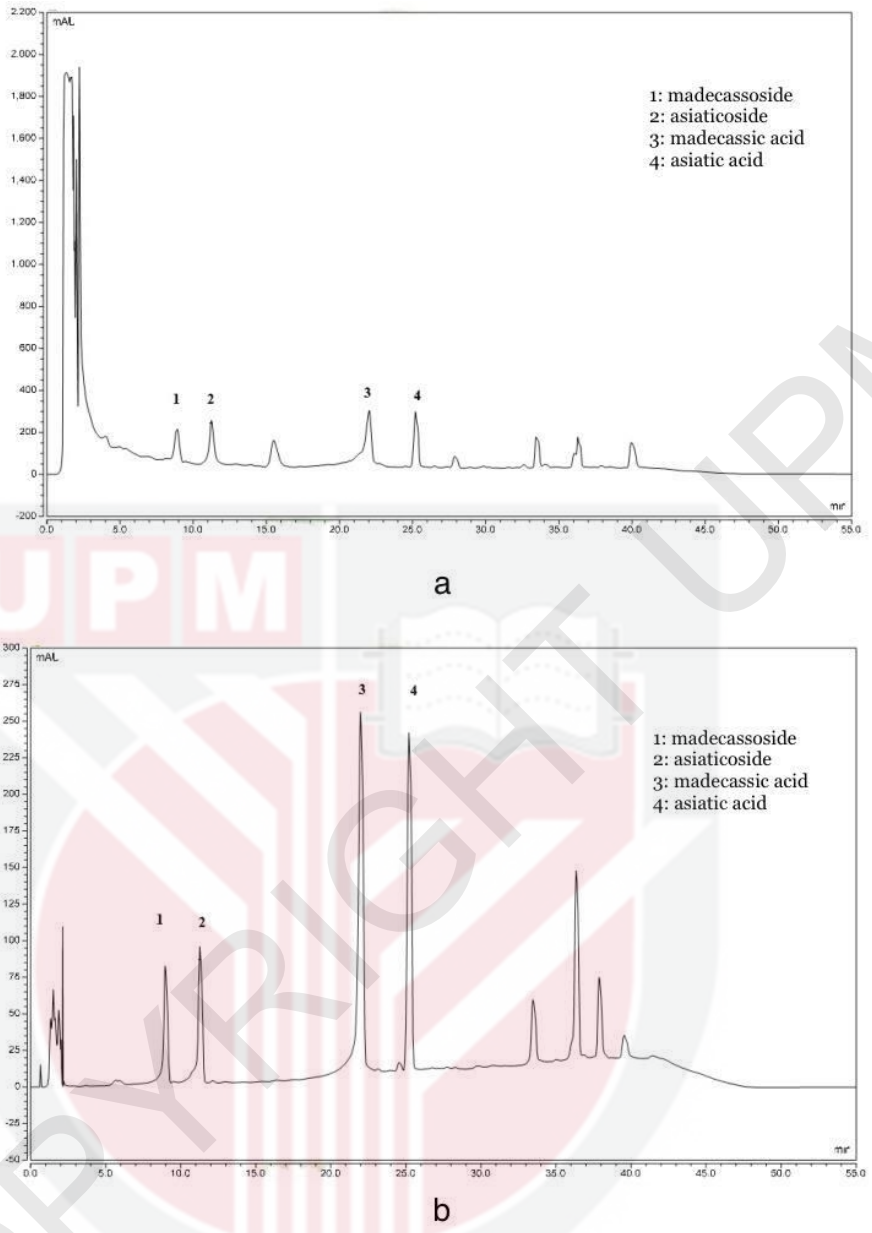

Figure 2.9: High-performance liquid chromatography (HPLC) analysis of (a) ethanolic extract of *Centella asiatica* and (b) standards mixture. The highest proportion of triterpenes is madecassoside, followed by asiaticoside, while the lowest is asiatic acid. Adapted from Hafiz et al. (2020).

2.4.3 Therapeutic potentials of *Centella asiatica*

CA, HB and HS all belong to the genus Centella and Hydrocotyle of the Apiaceae family (Maulidiani et al., 2012). Among the three *pegaga* varieties, CA is the most preferred species by scientists as it has the highest antioxidant level (Maulidiani et al., 2014). Analysis of total phenolic content (TPC) found CA to have

the most abundant phenolic compounds, underlining the free radical scavenging activity. This suggests a potential contribution of CA in the treatment of ND. The TPC analysis is as follows: CA (72.09 mg/100 g DW), HB (28.55 mg/100 g DW) and HS (56.23 mg/100 g DW). Similarly, Hashim et al. (2011) reported that CA exhibits a notable free radical scavenging activity, likely contributed by the high level of asiaticoside.

Various publications have named CA a herb that can ameliorate ND (Gregory et al., 2021; Hussin et al., 2020; Yogeswaran et al., 2016). For example, it is suggested that CA mediates improvements in neuronal health and cognition by decreasing oxidative stress, thus making it a potential neuroenhancement adjunct for treating AD (Matthews et al., 2019). The association of CA with cognitive functions is further demonstrated in rodents that recorded better performance in learning and memory upon oral administration of CA (Wong et al., 2019). There is a marked decrease in the levels of Aβ1–40 and Aβ1–42 located in the hippocampus following administration with CA; therefore, it may be valuable to incorporate CA in the treatment regime for AD (Dhanasekaran et al., 2009). Moreover, amyloid plaques are reduced as a result of treatment of a higher dose of CA in the long term. On the other hand, the triterpenes components in this herb may deliver protection against the damaging UV ray (Hashim et al., 2011).

Hafiz et al. (2020) presented an insight into the effect of ethanolic extract of CA (EECA) in rats suffering from AD. Cytotoxicity tests done on different concentrations of EECA ranging from 3.91 µg/mL to 1000 µg/mL found no cytotoxic effects in neuroblastoma cells and murine microglia cells. Next, it is noted that EECA

promotes suppression of pro-inflammatory cytokines and oxidative stress activities both in vivo and in vitro. Besides, prevention in acetylcholinesterase activities is linked to a potential elevation of acetylcholine which is significantly depleted in AD patients. An increase in neurotransmitters can improve the transmission of synapses in the hippocampus and cerebral cortex.

Apart from that, neuroprotective and antioxidant properties of asiatic acid play essential roles in overcoming neurodegeneration in hippocampus as seen in rat models (Welbat et al., 2018). Through neuroprotection effect, CA is presumed to be helpful in treating ND as it can protect nerve cells from death (Yogeswaran et al., 2016). Neuroregeneration is also documented: in the presence of NGF, EECA causes a significant increase in neurite outgrowth in rats which provides relevance in accelerating repair of damaged nerve cells (Soumyanath et al., 2005). On this basis, there is a prospect of CA in offering a wide range of therapeutic values as an enhancer in acellular therapy for ND.

2.4.4 Neuroenhancement properties of *Centella asiatica* on the production of stem cells derived-exosomes

CA's role as a natural product mediating acellular therapy has been scientifically investigated. A preliminary study by Nordin et al. (unpublished, 2021) aimed to unravel the potential of CA as an enhancer to produce good quality stem cells-derived exosomes. The effect of CA extract on the production of BDNF secreted by AFSCs has been assessed. EECA was introduced in R3 undergoing transdifferentiation into NSCs. As a result, it is interestingly discovered that CA promoted higher production of BDNF in the secretomes of R3 undergoing transdifferentiation into NSCs as compared to the untreated group. The increased level

of secreted BDNF upon treatment with CA is associated with neuroenhancement effect.

Altogether, neuroprotective properties of CA are evident through the enhancement of stem cells-derived exosomes that carry valuable NF essential for neuronal development. As such, these findings offer a window on the applications of CA as it is reputed to exert antibacterial, antifungal, antidepressant, antiepileptic, antinociceptive, antioxidant and anti-inflammatory properties (Gohil et al., 2010; Ullah et al., 2009; Welbat et al., 2018). Therefore, an effort to translate acellular therapy into clinical practice should be undertaken to overcome the limitations of conventional treatments of ND and hopefully serves as a better option than cellular therapy in the future.

CHAPTER 3

MATERIALS AND METHODS

3.1 Study design

Stem cell line used in this study was (R3) established in-house by Assoc. Prof. Dr. Norshariza Nordin and colleagues (Mun Fun et al., 2015). Three batches of R3 were used: P36, P38 and P40. This study aims to investigate three specific objectives as shown in Figure 3.1.

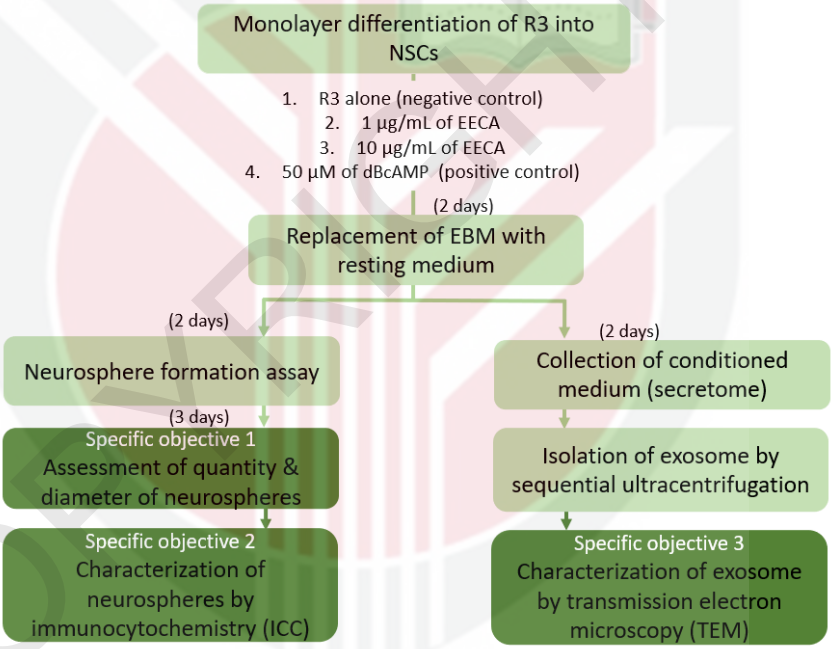

Figure 3.1: Methodologies of study. Schematic flow diagram of the methodologies is illustrated with the specific objectives.

Our study focuses on isolation of exosomes by sequential ultracentrifugation, neurosphere formation and characterization of exosomes by TEM (Figure 3.2).

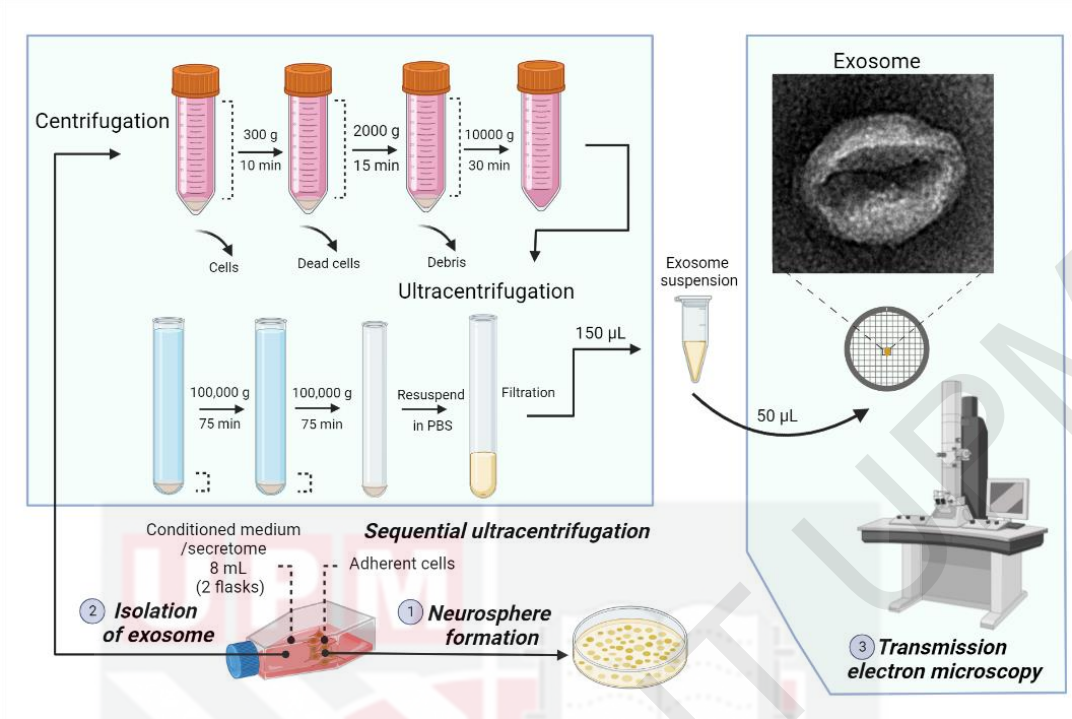

Figure 3.2: Study design. The methodologies include isolation of exosomes by sequential ultracentrifugation, neurosphere formation and characterization of exosomes by TEM.

3.2 Ethanolic extract of *Centella asiatica* (EECA)

Powdered form of EECA was provided by Prof Dr. Mohd Ilham Adenan (Universiti Teknologi MARA). The powder was reconstituted with sterile water at the concentration of 1 µg/mL and 10 µg/mL.

3.3 Cell Culture

3.3.1 Routine cell culture work

Cell culture works were carried out in Class II Biosafety Cabinet (BSC; BioAir, EuroClone, Italy). Appropriate sterilization procedure was performed prior the operation of BSC. Cell culture wastes were soaked and washed with 5% Virkon, then autoclaved before disposal. R3 was maintained in embryonic stem cells medium

(ESM) consisting of 1X Glasgow Minimum Essential Medium (GMEM; Gibco, Thermo Fisher Scientific, USA), 7.5% sodium bicarbonate (Gibco, Thermo Fisher Scientific, USA), 1 mM sodium pyruvate (Gibco, Thermo Fisher Scientific, USA), 2 mM L-glutamate (Gibco, Thermo Fisher Scientific, USA), 0.1 mM 2-mercaptoethanol (Gibco, Thermo Fisher Scientific, USA), 15% fetal bovine serum (FBS; Gibco, Thermo Fisher Scientific, Brazil). 20 ng/mL leukemia inhibitory factor (LIF; Gibco, Thermo Fisher Scientific) was added into the ESM to maintain the undifferentiated state of the cells.

3.3.2 Thawing of R3

Cryovials containing the cryopreserved R3 were retrieved from -80°C freezer or liquid nitrogen tank, then gently and quickly swirled in 37°C water bath. 1 mL of ESM was added into the cryovials to revive the cells. Cell suspension was transferred into a 15 mL centrifuge tube filled with an appropriate amount of ESM. The cells were centrifuged at 1000 rpm (Centrifuge DSC-301SD; Yihder Technology, Taiwan) for 5 minutes to remove DM SO residues. Following centrifugation, the supernatant was removed and the cell pellet was gently resuspended in an appropriate amount of ESM. Then, the cells were transferred into a 0.1% gelatin-coated T25 culture flask (Nunc, Thermo Fisher Scientific). Cells were incubated in a 5% CO_2, 37°C incubator.

3.3.3 Cells observation using inverted microscope

The flask containing cells was placed on the stage of an inverted microscope (Olympus). Observation of cells was made starting with the lowest magnification, 4X. Light intensity and condenser were adjusted accordingly. Images viewed under the microscope were produced by adjusting the coarse and fine adjustment knobs. Cells

observation was made every 2 days or as necessary to monitor the cells' state and confluency.

3.3.4 Culture and maintenance of cells

R3 was cultured in T25 flask. The culture medium was changed every 2 days. Once the cells reached a confluency of 70 - 90%, the cells were subcultured. The cells in the flask were washed twice with 1X phosphate buffer solution (PBS; Gibco, Thermo Fisher Scientific, USA), trypsinized using 0.25% Trypsin-EDTA (Gibco, Thermo Fisher Scientific, Canada) followed by incubation at room temperature for 2-3 minutes to allow cells detachment from the surface of the flask. The trypsin activity was deactivated with the addition of FBS (Gibco, Thermo Fisher Scientific, Brazil). The cell suspension was then transferred into a 15 mL centrifuge tube and centrifuged at 1000 rpm (Centrifuge DSC-301SD; Yihder Technology, Taiwan) for 5 minutes. Supernatant was carefully removed and the pellet was resuspended in 2-3 mL ESM. Cell seeding density was quantified using a hemocytometer under an inverted microscope. The cells were then seeded into a 0.1% gelatin-coated T25 flasks at the seeding density of 3.0×10^4 cells/cm^2 and incubated in 5% CO_2, 37°C incubator.

3.3.5 Counting of cells

Cell enumeration was performed after trypsinization of cells by transferring 10 µL of trypan blue (Sigma-Aldrich) onto a parafilm. Subsequently, 10 µL of cell suspension was resuspended with the trypan blue to stain the cells. The mixture was transferred onto a hemocytometer to be viewed under inverted microscope. Shining colorless cells were counted as viable cells, as opposed to the dead cells stained in blue that have absorbed the trypan blue dye. The cells were seeded in T25 culture flasks at

the density of 10 000 cells/cm². The total number of viable cells was calculated as follows:

$$\text{Viable cells/mL} = \frac{\text{total cells counted on the grid}}{4} \times 10^4 \times \text{volume of cell suspension} \times \text{dilution factor}$$

3.3.6 Cryopreservation of cells

After cell counting was performed, 900 µL of media containing 1×10^6 cells were transferred into cryovials. Then, 100 µL of DMSO was added into the cryovials. Cryovials were stored in -80°C freezer for short-term storage.

3.3.7 NSCs induction

R3 was transdifferentiated into NSCs through monolayer differentiation. NSC induction medium used is Embryoid Body Medium (EBM) which is similar to ESM in the absence of LIF: GMEM (Gibco, Thermo Fisher Scientific), 7.5% sodium bicarbonate (Gibco, Thermo Fisher Scientific), 1 mM sodium pyruvate, 2 mM L-glutamate (Gibco, Thermo Fisher Scientific), 0.1 mM 2-mercaptoethanol (Gibco, Thermo Fisher Scientific), and 10% FBS (Gibco, Thermo Fisher Scientific). Trypsinized R3 cells were cultured in EBM in T25 flasks (2 flasks for each group). The treatment groups were R3 treated with EECA at 1 µg/mL and 10 µg/mL, while negative control used R3 alone and positive control used R3 treated with 50 µM of dBcAMP (dibutyryl-cAMP) as shown in Table 3.1. All cells were incubated in 5% CO_2, 37°C incubator for 2 days to allow the transdifferentiation of R3 into NSCs.

Table 3.1: Group for monolayer differentiation of R3 into NSCs

Group	Type	Remark
Untreated	Negative control	R3 alone
1 μg/mL EECA	Treatment	R3 treated with 1 μg/mL of EECA
10 μg/mL EECA	Treatment	R3 treated with 10 μg/mL of EECA
50 μM dBcAMP	Positive control	R3 treated with 50 μM of dBcAMP

3.3.8 Resting stage of NSCs in DMEM/F12

After 2 days of NSCs induction, the EBM in all groups was replaced with a resting medium made of 1X Nutrient Mixture F-12 (DMEM/F12; Gibco, Thermo Fisher Scientific, USA) supplemented with (1:1) 1X N-2 supplement (Gibco, Thermo Fisher Scientific, USA).

3.3.9 Neurosphere formation assay

The post-rest NSCs derived from R3 were trypsinized and plated in 100 mm uncoated bacteriological petri dish according to the respective groups (as in Table 3.1). The cells were seeded at 3.0×10^4 cells/cm² in neurosphere medium. Neurosphere medium contained 1X Neurobasal™ Medium (Gibco, Thermo Fisher Scientific, USA) supplemented with 1X B-27™ Plus Supplement (Gibco, Thermo Fisher Scientific, USA), 20 ng/mL Epidermal Growth Factor (EGF) Recombinant Human (Gibco, Thermo Fisher Scientific, USA), 20 ng/mL Basic Fibroblast Growth Factor (bFGF; Gibco, Thermo Fisher Scientific, USA), 1% of L-glutamine (Gibco, Thermo Fisher Scientific), and 2% of antibiotic-antimycotic (Gibco, Thermo Fisher Scientific, USA). The cells were incubated in 5% CO_2, 37°C incubator.

3.3.9.1 Analysis of the quantity and diameter of neurospheres

The formation of neurospheres was observed and analyzed after 3 days of incubation. Neurospheres were imaged under a fluorescence microscope (Olympus), then quantified and measured in terms of diameter (µm) using ImageJ software.

3.3.10 Immunocytochemistry (ICC) of neurospheres

Characterization of neurospheres was performed using a semi-quantitative method, ICC. The expression of NSC marker, nestin by the neurospheres was assessed. Table 3.2 describes the antibodies used.

Table 3.2: Antibodies for nestin marker

Primary antibody	Secondary antibody
N5413 anti-nestin produced in rabbit (1:200) (Sigma-Aldrich)	Alexa Fluor 488 goat anti-rabbit IgG (H+L) (1:200) (Invitrogen™)

The neurospheres were cultured in 24-well plates (TPP) for ICC procedure. After removal of medium, cells were gently rinsed with 1X PBS twice.

The cells were fixed with a fixative solution (4% paraformaldehyde, 1 M sodium hydroxide and 1x PBS) for 30 minutes at room temperature. The fixation solution was later removed, and cells were washed with 1X PBS three times to remove the chemical reagents.

Next, permeabilization of cells was performed by incubating the cells with a permeabilization solution (1% Triton-X-100 [Sigma-Aldrich, Merck KGaA] and 1X

PBS) for 15 minutes at room temperature. After removal of the permeabilization solution, the cells were again washed with 1X PBS thrice.

The cells were then incubated with a blocking solution (10% goat serum [Miilipore, Merck KGaA, USA], 1% bovine serum albumin [Sigma-Aldrich, Merck KGaA], 10% Tween 20 and 1X PBS) for 30 minutes at room temperature. Folowing removal of the blocking solution, the cells were washed with 1X PBS thrice. The cells were incubated with primary antibodies at the ratio of 1:200 at 4°C. After overnight incubation, the antibodies were removed and washed with 1X PBS thrice. Subsequently, secondary antibodies were added and incubated together with the cells in dark at room temperature. The antibodies were removed and washed with 1X PBS thrice. Next, nuclei were counterstained blue with 100 µL of 300 nM diluted 4',6-diamidino-2-phenylindole (DAPI; Gibco, Thermo Fisher Scientific, USA) blue staining solution for 10 minutes in dark at room temperature.

Finally, 1X PBS was added into each well containing the counterstained cells for hydration purpose prior to visualization. Immunostained neurospheres were imaged using an inverted fluorescence microscope (Olympus) and analyzed using ImageJ software.

3.3.10.1 Analysis of immunocytochemistry (ICC)

The fluorescent images of the stained neurospheres were analyzed by measuring the corrected total cell fluorescence (CTCF) on the expression of nestin marker. The measurement used values of the area, integrated density and mean gray value via ImageJ software as follows:

$$\text{CTCF} = \text{integrated density} - (\text{area of selected cell} \times \text{mean fluorescence of background readings})$$

3.4 Exosomes

3.4.1 Collection of conditioned medium (CM)

Two days following the replacement of EBM with resting medium (as in chapter 3.3.8), 8 mL of CM (secretomes, DMEM/F12) was collected from every group (2 flasks each). The CM of R3-derived NSCs was pooled according to the respective groups (as in Table 3.1) and transferred into Falcon tubes before being temporarily stored at 4°C for subsequent analysis.

3.4.2 Isolation of exosomes by sequential ultracentrifugation

CM of each group was centrifuged at 300 xg (Centrifuge DSC-301SD; Yihder Technology, Taiwan) for 10 minutes at 4°C; afterward, the pellet (containing cell debris) was discarded. Next, the supernatant was centrifuged at 2,000 xg for 15 minutes at 4°C and the pellet (containing cell debris) was discarded. Subsequently, the supernatant was centrifuged at 100,00 xg for 30 minutes at 4°C and the pellet (containing microvesicles or apoptotic bodies) was discarded. Using ultracentrifuge, (Optima L-100 XP; swinging bucket SW41 Ti rotor; Beckman Coulter, USA) the supernatant transferred into 14 mL centrifuge tubes (Ultra-Clear Tubes; Beckman Coulter, USA) and topped-up with ice-cold PBS to completely fill the tube was centrifuged at 140,000 xg for 1 hour 15 minutes at 4°C. The pellet (containing exosomes, small extracellular vesicles or contaminating proteins) was retrieved while the supernatant was transferred into 15 mL tube and stored in -80°C freezer. After washing of pellet with 12 mL of 1X ice-cold PBS, the pellet was centrifuged at 140,000

xg for another 1 hour 15 minutes at 4°C. The supernatant was transferred into 15 mL tube stored in -80°C freezer. Meanwhile, the pellet (containing exosomes) was resuspended in 150 μL 1X ice-cold PBS before being filtered with 0.22 μM PES hydrophilic syringe filters into Eppendorf tubes. Finally, the exosome suspension was temporarily stored at 4°C for TEM analysis.

3.4.3 Characterization of exosomes by transmission electron microscopy (TEM)

Firstly, 50 μL of samples (exosome suspension) obtained from sequential ultracentrifugation was dropped onto a piece of parafilm according to the respective groups. Next, 400-mesh formvar coated copper (FCF400-CU) grids were put onto each sample droplet at 25°C (room temperature) for 4-5 minutes. Yellow-colored 1% uranyl acetate droplets were dropped carefully onto the same piece of parafilm, side-by-side with the samples - bubbles in each droplet were removed (if any). FCF400-CU grids were transferred carefully from the sample droplets, and placed onto (i.e. negatively stained with) the uranyl acetate droplets using a clean forcep at room temperature for 4-5 minutes. Excess liquid was removed in which the grids (together with the samples) were 'dried' using a Whatman filter paper. The grids/samples were then observed using JEM-2100F TEM (JEOL Ltd.) operated at 200 kV. Images were obtained using Gatan Orius imaging software.

3.4.3.1 Analysis of exosomes

The exosomes isolated from the CM of R3-derived NSCs were analyzed by comparing the morphology between groups and measuring the diameters (length of biggest dimension) in nm using ImageJ software.

3.5 Statistical analysis

Data were analyzed using IBM SPSS Statistics 26.0 (64-bit version). One-way analysis of variance (ANOVA) followed by Tukey's post-hoc test analysis was carried out to compare the means of two or more groups. The p-value of less than 0.05 ($p<0.05$) was considered to have a significant result.

CHAPTER 4

RESULTS

4.1 Culture of R3

R3 culture in ESM exhibits cuboidal morphology (Figure 4.1). Each nucleus contains multiple nucleoli.

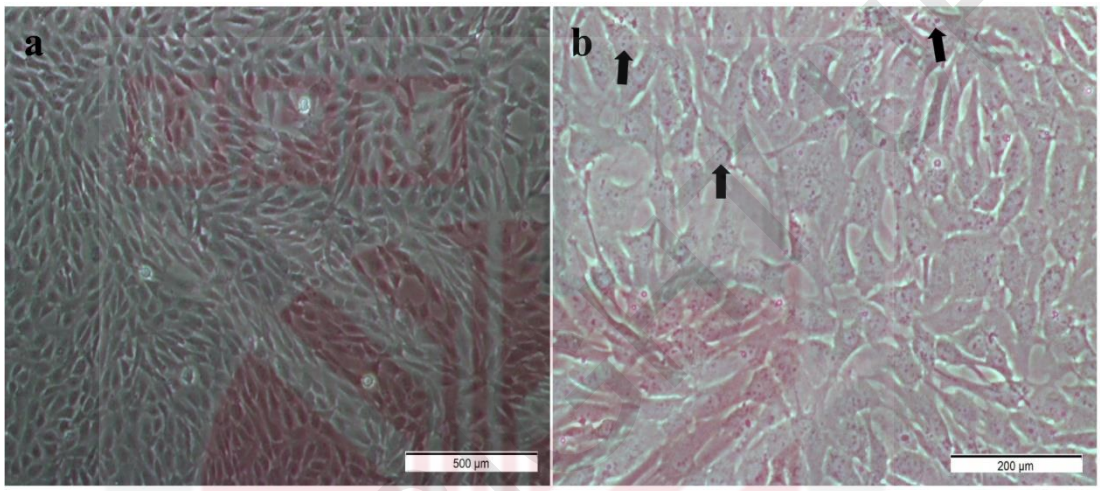

Figure 4.1: Culture and propagation of R3 on the day in vitro 10 (DIV10) grown in ESM. Images were viewed under the inverted microscope with 4X (**a**) and 10X (**b**) magnifications. Cells exhibit cuboidal-like morphology. Arrows show the multiple nucleoli in the nucleus of R3.

4.2 NSCs induction

Two days following NSCs induction, cells are shown to exhibit neural rosette formation (Figure 4.2). The cells show relatively similar morphological characteristics among all groups.

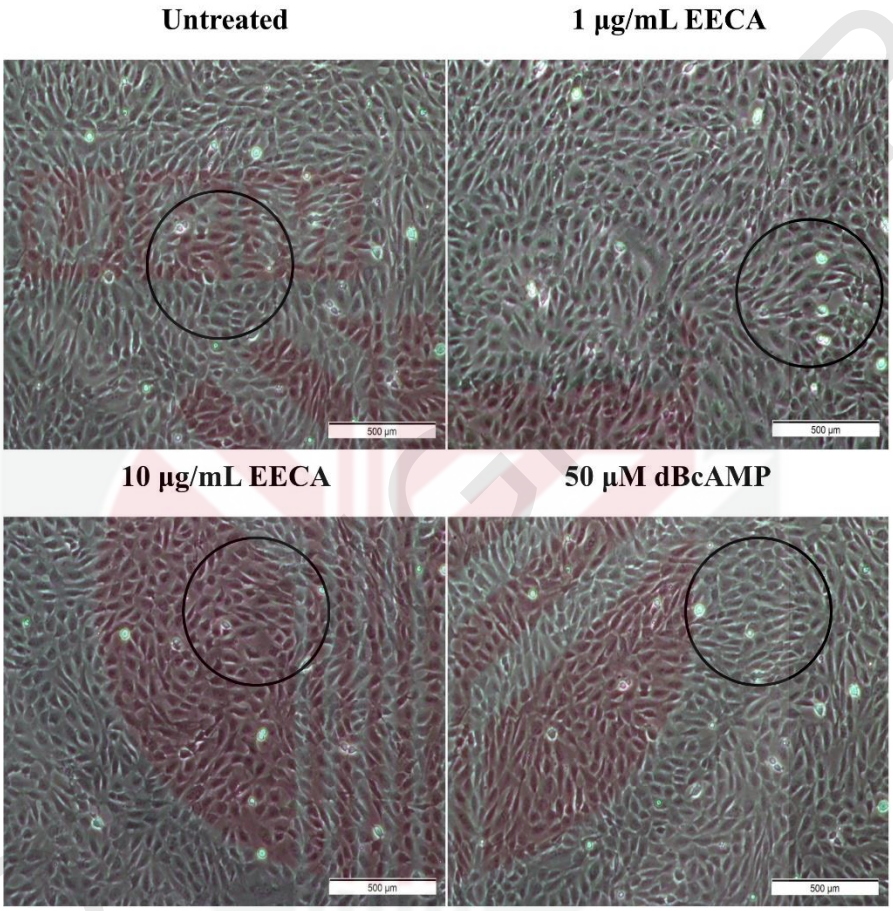

Figure 4.2: NSCs observed in each group under the inverted microscope on the DIV2 grown in EBM. Scale bar is 500 µm. Cells exhibit neural rosette formation (as represented by the circles).

4.3 Quantity and diameter of neurospheres

NSCs were grown in spherical aggregates known as neurospheres as in Figure 4.3. The morphology is consistent throughout all groups, and differ in term of size. All neurospheres were measured in nm using ImageJ, where results show a diversity in the diameters within and among groups. Based on Figure 4.4, the average diameter of

neurospheres formed in each group are as follows: Untreated (93.91 µm), 1 µg/mL EECA (86.82 µm), 10 µg/mL EECA (82.13 µm), and 50 µM dBcAMP (87.21 µm).

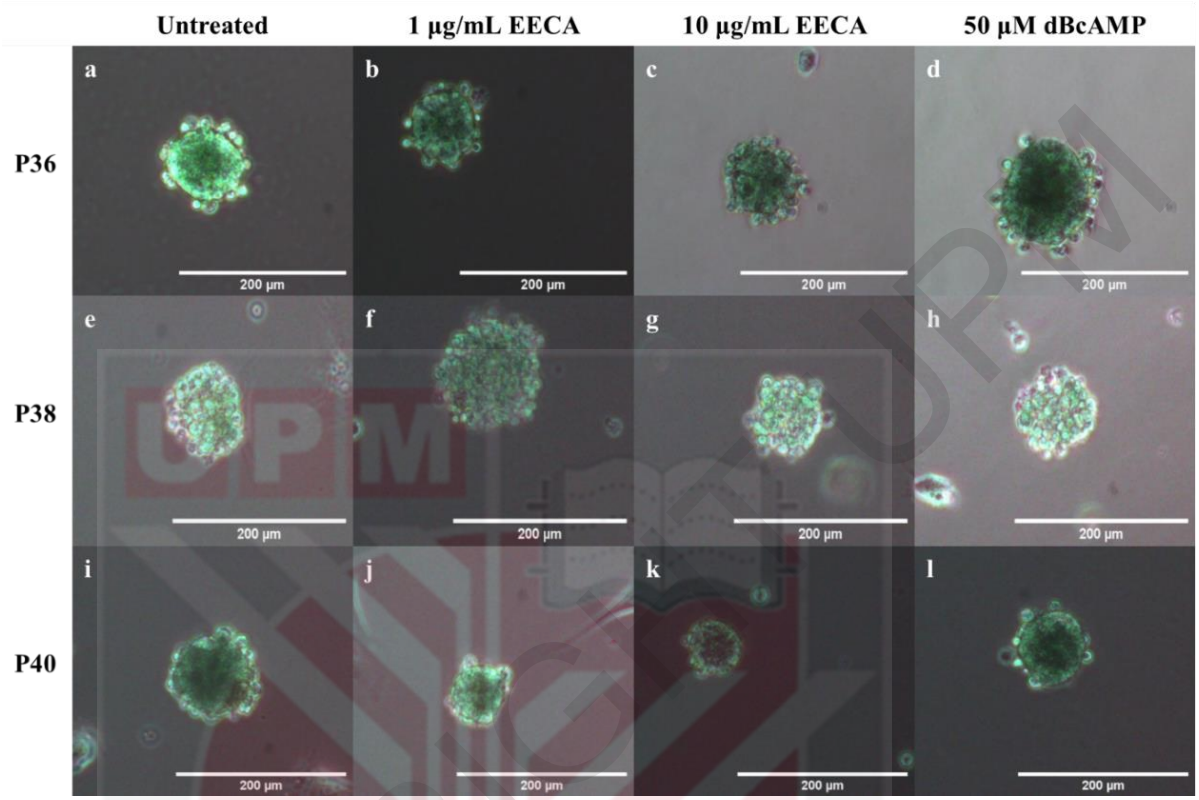

Figure 4.3: Neurospheres observed in each group under the inverted microscope on the DIV3. Neurospheres were grown in Neurobasal/B27 medium from three batches: P36 (**a-d**), P38 (**e-h**), and P40 (**i-l**). Scale bar is 200 µm.

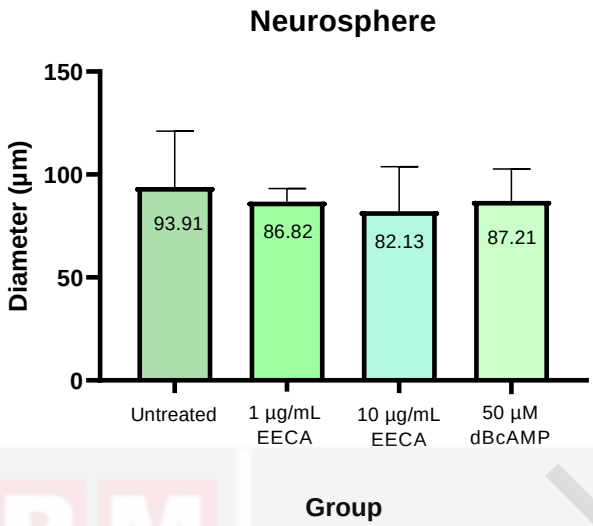

Figure 4.4: Bar graph illustration on the average diameter of neurospheres. Average diameter of neurospheres formed in each group varies. Error bars show the values of ± SD from two independent experiments, n=2 (7 to 95 neurospheres per group), one-way ANOVA.

Note: the statistical analysis was done for two independent experiments. The data for another independent experiment (P40 batch) can be found in Appendix B.

We further analyze the portion of neurospheres within the range of 50-100 µm in Figure 4.5. The percentages of neurospheres with the size of 50-100 µm is the highest in 1 µg/mL EECA (70%), followed by 10 µg/mL EECA (61%), 50 µM dBcAMP (58%) and Untreated (40%) group.

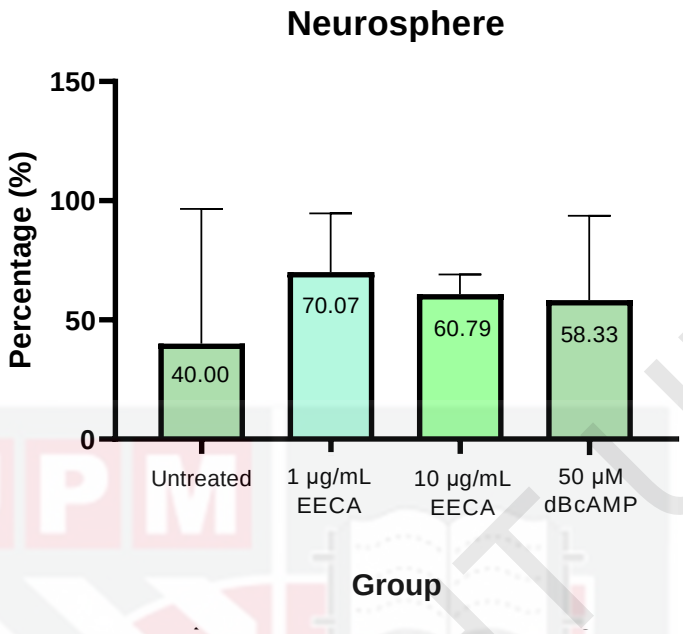

Figure 4.5: Bar graph illustration on the average percentage of 50-100 µm neurospheres in each group. The percentages are the highest in 1 µg/mL EECA (70%) and 10 µg/mL EECA (61%). Error bars show the values of ± SD from two independent experiments, n=2 (0 to 95 neurospheres per group), one-way ANOVA.

Note: the statistical analysis was done for two independent experiments. The data for another independent experiment (P40 batch) can be found in Appendix B.

4.4 Characterization of neurospheres by the expression of NSCs marker

Figure 4.6 displays that green fluorescence signals were detected by the following groups: Untreated, 1 µg/mL EECA and 50 µM dBcAMP. Unfortunately, signals from 10 µg/mL EECA failed to be detected due to technical error.

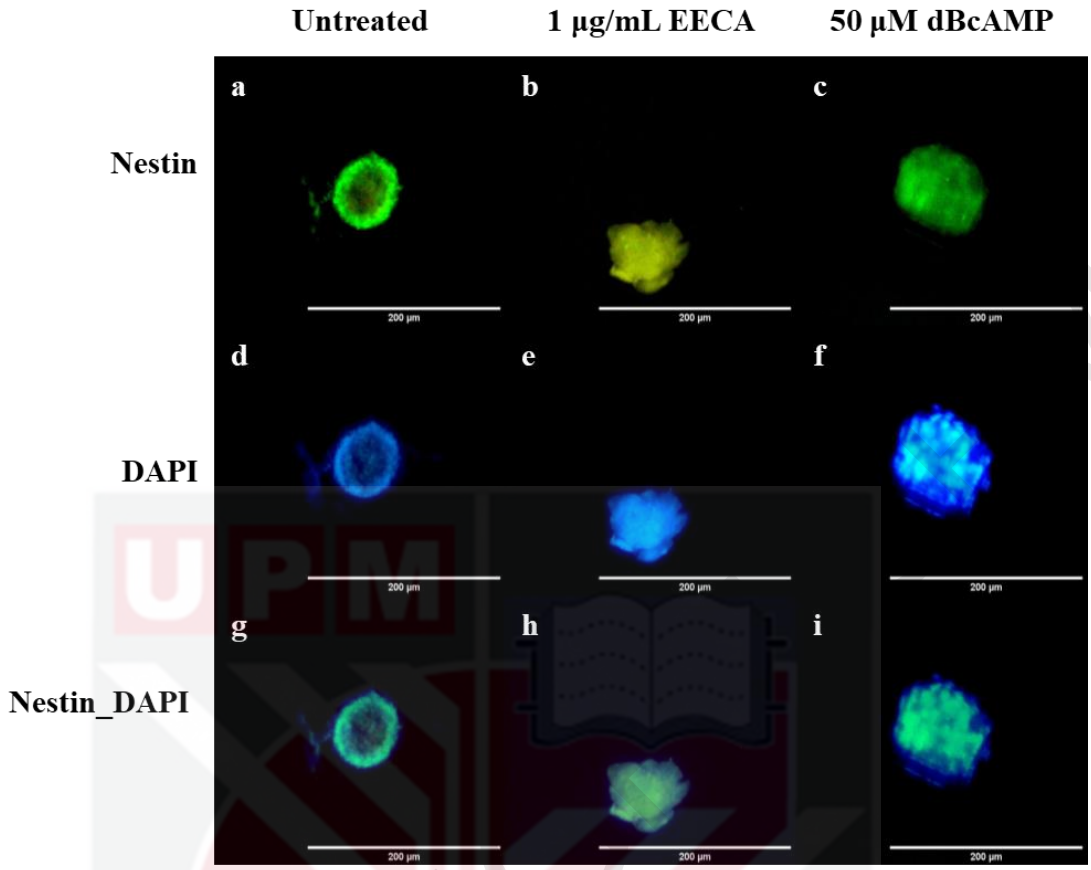

Figure 4.6: Immunocytochemistry (ICC) of neurospheres with nestin marker. ICC images of neurospheres stained with nestin (green) in each group: Untreated (**a**), 1 µg/mL EECA (**b**) and 50 µM dBcAMP (**c**). The nuclei are counterstained blue with DAPI (**d-f**), and merged form is presented in **g-i**. Observation is representative of batch P36. Scale bar is 200 µm.

Semi-quantitative analysis in Figure 4.7 shows that CTCF of 1 µg/mL EECA is higher (3.12) than the Untreated (2.85) and 50 µM dBcAMP groups (1.35). The statistical analysis shows no significant difference at $\alpha = 0.05$.

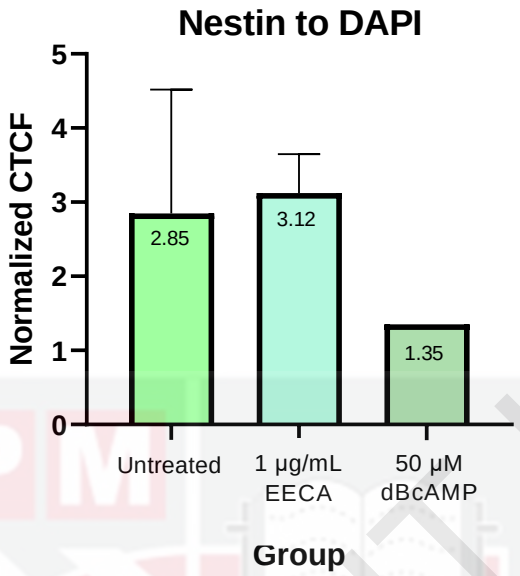

Figure 4.7: Bar graph illustration on the normalized corrected total cell fluorescence (CTCF) of nestin to DAPI in each group. CTCF of 1 µg/mL EECA is higher than the Untreated and 50 µM dBcAMP groups. Error bars show the values of ± SD from one independent experiment, n=1 (1 to 3 neurospheres per group), one-way ANOVA.

4.5 Characterization of exosomes

Exosomes were successfully isolated from the CM of R3-derived NSCs from two batches (P38 and P40) using sequential ultracentrifugation. Evaluation and characterization of the isolated exosomes of all groups were done using TEM.

Table 4.1 shows the exosomal yield (per 50 µL of sample) in each group following sequential ultracentrifugation for P38 and P40 batches. The data represent the quantity of exosomes isolated from 8 mL of CM pooled from two flasks of R3-derived NSCs containing 600,000 cells each. Note that the exosomes pellet formed following sequential ultracentrifugation was resuspended in 150 µL of ice-cold PBS prior to TEM analysis. Since the amount of exosome suspension sampled for TEM

analysis is one-third of the original amount, the total exosomal yield from the entire collected CM per flask should be thrice the number of exosomes observed under TEM.

Table 4.1: Exosomal yield in each group from two batches, P38 and P40

Group	Exosomal yield (per 50 µL of sample)	
	P38	P40
Untreated	3	18
1 µg/mL EECA	5	13
10 µg/mL EECA	1	11
50 µM dBcAMP	1	2

Through the negative staining method, membrane-bound vesicles of 50–150 nm were contrasted against the dark-colored background as shown in Figure 4.8. These nano-sized vesicles known as exosomes display a typical double-concave disc-like structure with a central depression. Their surface structure was visible under TEM as the vesicles were coated with heavy metal salts (Zabeo et al., 2017).

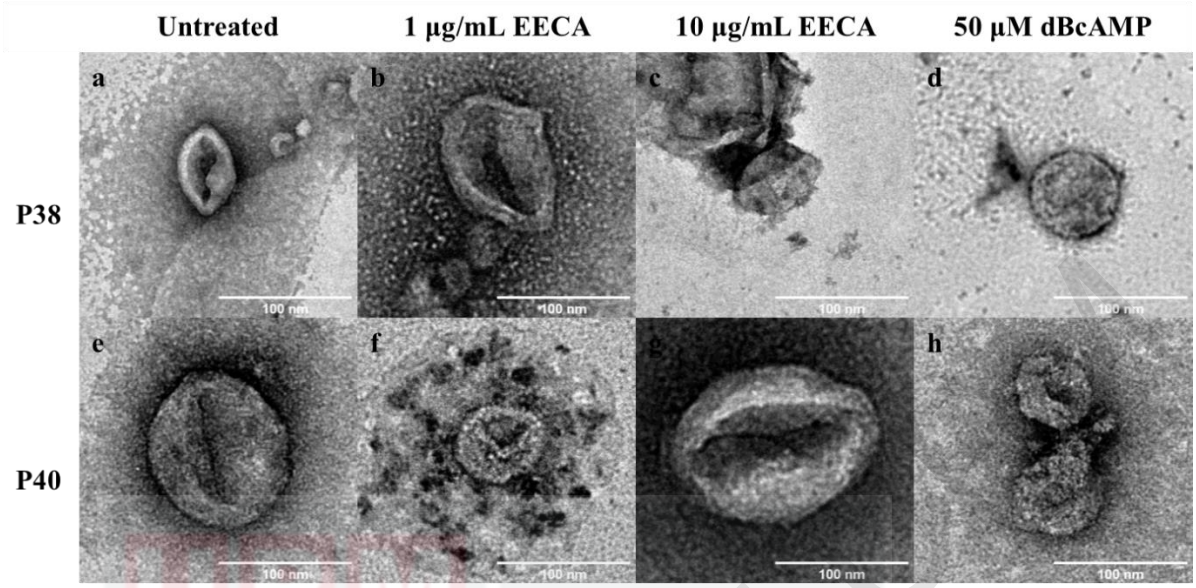

Figure 4.8: Exosomes observed in each group under the TEM. Exosomes were isolated from two batches: P38 (**a**-**d**) and P40 (**e**-**h**). Scale bar is 100 nm. Exosomes are characterized as single vesicles.

The average diameter of exosomes formed in each group are as follows: Untreated (79.30 nm), 1 µg/mL EECA (79.50 nm), 10 µg/mL EECA (114.83 nm), 50 µM dBcAMP (70.82 nm). Figure 4.9 illustrates that the average diameter of exosomes is not significantly different between groups at $\alpha = 0.05$.

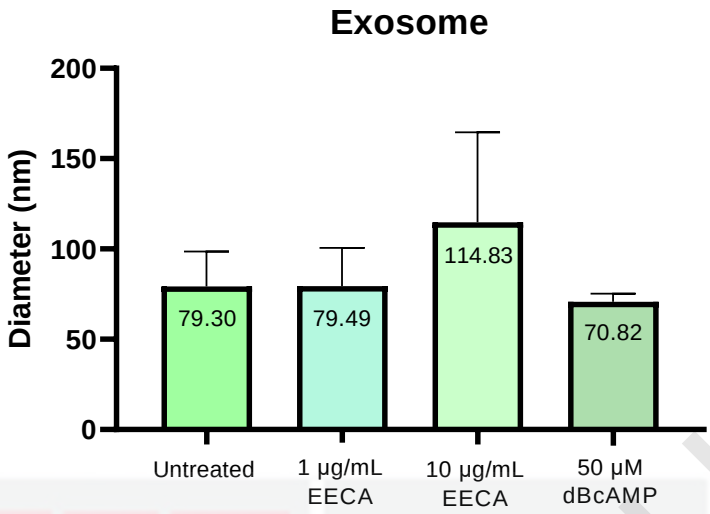

Figure 4.9: Bar graph illustration on the average diameter of exosomes. Average diameter of exosome formed in each group is in between 70 to 120 nm. Error bars show the values of ± SD from two independent experiments, n=2 (1 to 18 exosomes per group), one-way ANOVA.

Meanwhile, Figure 4.10 shows unique exosomal characteristics identified in 10 µg/mL EECA group from P40 batch, namely a protrusion-like appearance and an occurrence of a within-vesicle exosome.

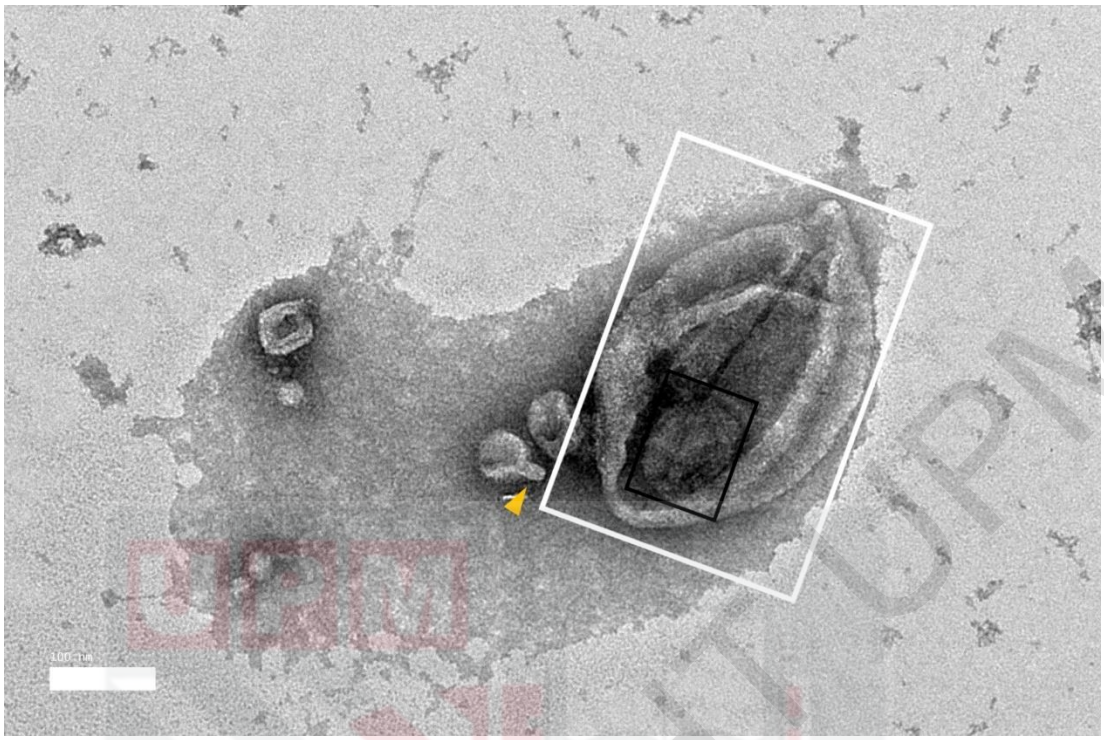

Figure 4.10: Exosomes observed in 10 µg/mL EECA group under the TEM. Image shows an exosome (in black box) contained in a bigger vesicle (in white box). Arrowhead (in yellow) points to protrusion-like appearance. Observation is representative of batch P40. Scale bar is 100 nm.

CHAPTER 5
DISCUSSION

5.1 Culture of R3

The identity of R3 cells was confirmed by the cuboidal-like morphology and presence of multiple nucleoli within the nucleus of the cells (Figure 4.1). The morphology is in accordance with c-kit positive cells isolated from full-term rat by Mun Fun et al. (2015).

5.2 NSCs induction

From Figure 4.2, we can observe rosette formation that represents early neural tube structures which form the brain (Shang et al., 2018). This validates the identity of the cells as a type of NSCs following the transdifferentiation from R3.

5.3 Quantity and diameter of neurospheres

NSCs were grown as neurospheres in Neurobasal /B27 medium. The formation of neurospheres in this study verifies the ability of R3 to be induced into NSCs. Each neurosphere is composed of neural progenitor cells and NSCs (Soares et al., 2021). While the neurospheres formed in the present study vary in size as explained in Figure 4.4, we acknowledge that the size is critical for cell survival and metabolism (Dan Ge, 2012). Increased neurosphere size results in inadequate nutrition delivery and metabolic waste elimination, leading to neurospheres death. Proliferative capability is reduced when the diameter exceeds 100 μm. On this basis, we define good quality neurospheres having the diameters of 50 to 100 μm.

Based on Figure 4.5, 70% of the neurospheres formed in 1 μg/mL EECA group is good-sized neurospheres while 61% of the neurospheres formed in 10 μg/mL EECA is in the good size range. In contrast, 50 μM dBcAMP and Untreated groups record lower generation of good-sized neuropsheres at 58% and 40%, respectively. We conclude that the majority of the neurospheres produced by R3-derived NSCs treated with EECA exhibit good proliferative size (50-100 μm). The insignificant statistical analysis is likely influenced by small-sized samples.

All in all, these findings suggest the ability of R3-derived NSCs treated with EECA to positively influence the quantity of R3-NSCs-derived neurospheres with good proliferative size.

5.4 Characterization of neurospheres by the expression of NSCs marker

Characterization of neurospheres was performed by ICC. The green fluorescence signals mark the expression of molecular marker, nestin. Nestin is an intermediate filament protein that is required for proper survival and proliferation of NSCs (Park et al., 2010). In agreement with Park and colleagues (2010), we found that cells forming the neurospheres in this present study are positive for nestin (Figure 4.6). This is true for all groups except 10 μg/mL EECA. We failed to detect the expression of nestin in 10 μg/mL EECA group due to technical error. Nevertheless, the result from 1 μg/mL EECA is thought to be representative of the treatment groups to a certain extent as both groups were subjected to the same treatment that only varied by concentration. Based on this assumption, we speculate that the neurospheres in 10 μg/mL EECA are nestin-positive as well.

The fluorescent images of the stained neurospheres were analyzed by CTCF as in Figure 4.7. CTCF of 1 μg/mL EECA is higher than the Untreated and 50 μM dBcAMP groups, although not significant. Higher expression of the NSC marker suggests that treatment of EECA may enhance the quality of the neurospheres through a higher expression of the nestin marker. However, it is important to note the sample size is not large enough to produce a significant finding. More independent experiments need to be employed to ascertain this hypothesis.

Ultimately, the presence of R3-derived NSCs in neurospheres was confirmed by the detection of fluorescence signals by the green-stained neurospheres, subsequently validating the successful transdifferentiation of R3 into NSCs.

5.5 Characterization of exosomes

Exosomes released by cells transport various cargo including nucleic acids, proteins, lipids and metabolites (Kalluri & LeBleu, 2020; Khatun et al., 2016). Exosomes originate from any type of cell- resembling their parental cell (Théry et al., 2002). As the research on the exosomes derived from NSCs is emerging, characterizing these exosomes would create a constructive foundation to the scientific community in revealing the valuable potential of exosomes for use in clinical practices.

Table 4.1 illustrates the exosomes yielded by sequential ultracentrifugation. Ideally, the exosomal yield should be elevated by increasing the volume of the CM for an improved analysis. We did not focus on quantifying exosomes using TEM as the instrument is employed for qualitative analysis of the exosomes. There exists possibility that imaging would only be applied to the samples adhered to the grid rather

than the entire volume (Théry et al., 2018). Quantitative analysis is therefore more feasible to be carried out by other methods such as via nanoparticle tracking analysis (NTA). This emerging method is capable of measuring motion of the nanoparticles in suspension based on Brownian motion, hence allowing the quantification of exosomes (Khatun et al., 2016).

Based on Figure 4.9, the average diameter of exosomes formed in each group is in between 70 to 120 nm. Characterization of exosomes in this study is limited to studying the surface instead of the in-depth visualization of the internal features. There is central depression in the exosomes, a trait known as an artifact resulting from sample preparation (Cross et al., 2016). We found that all exosomes exhibit a membrane bilayer characterized as a single vesicle (Figure 4.8).

A unique characteristic is observed in 10 μg/mL EECA group in which there is a protrusion-like appearance (pointed by arrowhead) in an exosome, as shown in Figure 4.10. The mechanism of this phenomenon is not understood but may be caused by the presence of protein with certain functions in the protrusion (Zabeo et al., 2017). Another interesting characteristic seen in the same group is the occurrence of an exosome (in black box) within a bigger vesicle (in white box). The large-sized (365 nm) structure likely belongs to the microvesicles category since the size exceeds 150 nm. These unique occurrences were not observed in other groups.

The single vesicles morphology is consistent throughout all four groups. No double (smaller vesicle contained in a larger one) or triple vesicles are identified. We also rule out other morphological types such as tubule vesicles (elongated dimension

with parallel membranes on both ends of the axis of symmetry). The tubular form was observed by Zabeo et al. (2017) in proximity of single vesicles form. A hypothesis proposed behind the diversity of the exosomal morphology links the role of membrane-associated protein like BAR (Bin, Amphiphysin, Rvs)-domain proteins, integral amphipathic composition, or phospholipid to the membrane shaping (Frost et al., 2008).

In essence, there is no great diversity in the exosomal morphology within and among all groups. All exosomes represent complete vesicles (uninterrupted/discontinuous membranes); thus, defect in exosomes is not evident. All exosomes and membranes appear intact and not ruptured. TEM observations reveal that exosomal structures were not compromised upon the treatment with EECA; hence, EECA does not negatively influence the quality of NSCs-derived exosomes. The results merit further investigations on EECA-enriched exosomes as potential treatments for ND, especially in promoting neuroregeneration.

CHAPTER 6

CONCLUSION, LIMITATIONS AND RECOMMENDATIONS FOR FUTURE RESEARCH

6.1 Conclusion

The formation of neurospheres and the expression of NSC marker (nestin) confirm the successful transdifferentiation of R3 into NSCs. This justifies the relevance of using non-brain sources, that is by transdifferentiating AFSCs into NSCs in vitro to eliminate the invasive procedures of isolating NSCs from the brain. Although there is no certainty, the treatment of EECA may positively influence the quality and quantity of R3-NSCs-derived neurospheres. Importantly, EECA-enriched exosomal structures were not compromised upon the treatment with EECA, hence further in-depth investigation is worth pursuing. These findings suggest the use of EECA as the prospective neuroenhancement adjunct in generating good quality exosomes loaded with therapeutic cargos essential for acellular therapy against ND.

6.2 Limitations

The present data give the idea that the treatment of EECA may positively influence the production of neurospheres generated from R3-derived NSCs. However, based on the statistical analysis, none of the quantitative analyses produce a significant result for a certain conclusion to be made. We speculate that this is due to the small sample size and an insufficient number of independent experiments.

6.3 Recommendations for future research

A crucial aspect that must be considered in conducting research is to produce a statistically significant result. For this reason, the number of biological replications should be increased. Another recommendation is to quantify the expression of NSC markers using flow cytometry for more reliable data. Other than that, characterize R3-derived NSCs in neurospheres via the expression of more NSC markers like Sox1 and Sox2. The subsequent direction of this project would be performing advanced analyses to quantitatively and qualitatively characterize exosomes via NTA. Finally, investigation of cargos carried by exosomes should be performed to further understand the effect of EECA on the therapeutic values of exosomes.

REFERENCES

Arrigo, D. D., Ro, A., Cucchiarini, M., Moretti, M., Candrian, C., & Filardo, G. (2019). Secretome and Extracellular Vesicles as New Biological Therapies for Knee Osteoarthritis : A Systematic Review. *Journal of clinical medicine, 8(11), 1867.* https://doi.org/10.3390/jcm8111867

Casarosa, S., Bozzi, Y., & Conti, L. (2014). Neural stem cells : ready for therapeutic applications ? *Molecular and cellular therapies, 2, 31*. https://doi.org/10.1186/2052-8426-2-31

Chung, C. C., Huang, P. H., Chan, L., Chen, J. H., Chien, L. N., & Hong, C. T. (2020). Plasma Exosomal Brain-Derived Neurotrophic Factor Correlated with the Postural Instability and Gait Disturbance–Related Motor Symptoms in Patients with Parkinson's Disease. *Diagnostics*, *10*(9). https://doi.org/10.3390/diagnostics10090684

Cross, Sarah J. Linker, Kay E. Leslie, F. M. (2016). 乳鼠心肌提取 HHS Public Access. *Physiology & Behavior*, *176*(1), 100–106. https://doi.org/10.1039/c5an00688k.Exosomes

Dan Ge. (2012). Effect of the neurosphere size on the viability and metabolism of neural stem/progenitor cells. *African Journal of Biotechnology*, *11*(17), 3976–3985. https://doi.org/10.5897/ajb11.3324

De Coppi, P., Bartsch, G., Siddiqui, M. M., Xu, T., Santos, C. C., Perin, L., Mostoslavsky, G., Serre, A. C., Snyder, E. Y., Yoo, J. J., Furth, M. E., Soker, S., & Atala, A. (2007). Isolation of amniotic stem cell lines with potential for therapy. *Nature Biotechnology*, *25*(1), 100–106. https://doi.org/10.1038/nbt1274

De Gioia, R., Biella, F., Citterio, G., Rizzo, F., Abati, E., Nizzardo, M., Bresolin, N., Comi, G. Pietro, & Corti, S. (2020). Neural stem cell transplantation for neurodegenerative diseases. *International Journal of Molecular Sciences*, *21*(9). https://doi.org/10.3390/ijms21093103

Dhanasekaran, M., Holcomb, L. A., Hitt, A. R., Tharakan, B., Porter, J. W., Young, K. A., & Manyam, B. V. (2009). *Centella asiatica Extract Selectively Decreases Amyloid β Levels in Hippocampus of Alzheimer ' s Disease Animal Model*. *19*(December 2008), 14–19. https://doi.org/10.1002/ptr

Ding, W. Y., Huang, J., & Wang, H. (2020). Waking up quiescent neural stem cells: Molecular mechanisms and implications in neurodevelopmental disorders. *PLoS Genetics*, *16*(4), 1–26. https://doi.org/10.1371/journal.pgen.1008653

Frost, A., Perera, R., Roux, A., Spasov, K., Destaing, O., Egelman, E. H., De Camilli, P., & Unger, V. M. (2008). Structural Basis of Membrane Invagination by F-BAR Domains. *Cell*, *132*(5), 807–817. https://doi.org/10.1016/j.cell.2007.12.041

Gohil, K. J., Patel, J. A., & Gajjar, A. K. (2010). Pharmacological review on Centella asiatica: A potential herbal cure-all. *Indian Journal of Pharmaceutical Sciences*, *72*(5), 546–556. https://doi.org/10.4103/0250-474X.78519

Goncalves, J. T., Schafer, S. T., & Gage, F. H. (2016). *Review Adult Neurogenesis in the Hippocampus : From Stem Cells to Behavior*. 897–914. https://doi.org/10.1016/j.cell.2016.10.021

Govindan, G., Sambandan, T. G., Govindan, M., & Sinskey, A. (2007). *A Bioactive Polyacetylene Compound Isolated from Centella asiatica*. 4–6. https://doi.org/10.1055/s-2007-981521

Gregory, J., Vengalasetti, Y. V, Bredesen, D. E., & Rao, R. V. (2021). Neuroprotective Herbs for the Management of Alzheimer ' s Disease. *Biomolecules, 11(4)*, 543. https://doi.org/10.3390/biom11040543 1–19

Grochowski, C., & Maciejewski, R. (2018). *Neural stem cell therapy — Brief review*. *173*(July), 8–14. https://doi.org/10.1016/j.clineuro.2018.07.013

Hafiz, Z. Z., Mohd Amin, M. A., Johari James, R. M., Teh, L. K., Salleh, M. Z., & Adenan, M. I. (2020). Inhibitory Effects of Raw-Extract Centella asiatica (RECA) on Acetylcholinesterase, Inflammations, and Oxidative Stress Activities via in Vitro and in Vivo. *Molecules*, *25*(4). https://doi.org/10.3390/molecules25040892

Hamid, A. A., Khair, M., Mun-fun, H., Nurusaadah, S., Rejali, Z., Nazri, M., Thilakavathy, K., & Nordin, N. (2017). Highly potent stem cells from full-term amniotic fl uid : A realistic perspective. *Phytochemistry Letters*, *17*(1), 9–18. https://doi.org/10.1016/j.repbio.2017.02.001

Hashim, P., Sidek, H., Helan, M. H. M., Sabery, A., Palanisamy, U. D., & Ilham, M. (2011). Triterpene composition and bioactivities of centella asiatica. *Molecules*, *16*(2), 1310–1322. https://doi.org/10.3390/molecules16021310

Huang, X., Mao, Y. S., Li, C., Wang, H., & Ji, J. L. (2014). Venlafaxine inhibits apoptosis of hippocampal neurons by up-regulating brain-derived neurotrophic factor in a rat depression model. *Pharmazie*, *69*(12), 909–916. https://doi.org/10.1691/ph.2014.4661

Hussin, H. M., Lawi, M. M., Haflah, N. H. M., Kassim, A. Y. M., Idrus, R. B. H., & Lokanathan, Y. (2020). Centella asiatica (L.)-Neurodifferentiated Mesenchymal Stem Cells Promote the Regeneration of Peripheral Nerve. *Tissue Engineering and Regenerative Medicine*, *17*(2), 237–251. https://doi.org/10.1007/s13770-019-00235-6

Jonsson, S., Wiberg, R., McGrath, A. M., Novikov, L. N., Wiberg, M., Novikova, L. N., & Kingham, P. J. (2013). Effect of Delayed Peripheral Nerve Repair on Nerve Regeneration, Schwann Cell Function and Target Muscle Recovery. *PLoS ONE*, *8*(2). https://doi.org/10.1371/journal.pone.0056484

JPND. Retrieved January 23, 2022 from JPND Neurodegenerative Disease Research website: https://www.neurodegenerationresearch.eu/what/#:~:text=Dementias%20are%20responsible%20for%20the%20greatest%20burden%20of

Kalluri, R., & LeBleu, V. S. (2020). The biology, function, and biomedical

applications of exosomes. *Science*, *367*(6478), 139–148. https://doi.org/10.1126/science.aau6977

Kandoi, S., Praveen, L., Patra, B., & Vidyasekar, P. (2018). Evaluation of platelet lysate as a substitute for FBS in explant and enzymatic isolation methods of human umbilical cord MSCs. *Scientific Reports*, *April*, 1–12. https://doi.org/10.1038/s41598-018-30772-4

Khatun, Z., Bhat, A., Sharma, S., & Sharma, A. (2016). Elucidating diversity of exosomes: Biophysical and molecular characterization methods. *Nanomedicine*, *11*(17), 2359–2377. https://doi.org/10.2217/nnm-2016-0192

Kolios, G., & Moodley, Y. (2012). Introduction to stem cells and regenerative medicine. *Respiration*, *85*(1), 3–10. https://doi.org/10.1159/000345615

Li, P., Kaslan, M., Lee, S. H., Yao, J., & Gao, Z. (2017). Progress in exosome isolation techniques. *Theranostics*, *7*(3), 789–804. https://doi.org/10.7150/thno.18133

Li, Y. (2020). *Neural Stem Cell Niche and Adult Neurogenesis*. https://doi.org/10.1177/1073858420939034

Long, Q., Upadhya, D., Hattiangady, B., Kim, D., Yeon, S., & Shuai, B. (2017). *Intranasal MSC-derived A1-exosomes ease inflammation , and prevent abnormal neurogenesis and memory dysfunction after status epilepticus*. https://doi.org/10.1073/pnas.1703920114

Maguire, G. (2014). Stem cell therapy without the cells. *Communicative & integrative biology*, *6(6), e26631*. https://doi.org/10.4161/cib.26631

Matthews, D. G., Caruso, M., Murchison, C. F., Zhu, J. Y., Wright, K. M., Harris, C. J., Gray, N. E., Quinn, J. F., & Soumyanath, A. (2019). Centella asiatica improves memory and promotes antioxidative signaling in 5XFAD mice. *Antioxidants*, *8*(12). https://doi.org/10.3390/antiox8120630

Maulidiani, Abas, F., Khatib, A., Shaari, K., & Lajis, N. H. (2014). Chemical characterization and antioxidant activity of three medicinal Apiaceae species. *Industrial Crops and Products*, *55*, 238–247. https://doi.org/10.1016/j.indcrop.2014.02.013

Maulidiani, H., Khatib, A., Shaari, K., Abas, F., Shitan, M., Kneer, R., Neto, V., & Lajis, N. H. (2012). Discrimination of Three Pegaga (Centella) Varieties and Determination of Growth-Lighting Effects on Metabolites Content. *J. Agric. Food Chem. 2012, 60, 1, 410–417* https://doi.org/10.1021/jf200270y

Merck. *Neural Stem Cell Culture Protocols.* Retrieved April 25, 2022, from http://www.sigmaaldrich.com/technical-documents/protocols/biology/neural-stem-cell-culture-protocols.html

Mun-Fun, H., Ferdaos, N., Hamzah, S. N., Ridzuan, N., Hisham, N. A., Abdullah, S., Ramasamy, R., Cheah, P. S., Thilakavathy, K., Yazid, M. N., & Nordin, N. (2015). Rat full term amniotic fluid harbors highly potent stem cells. *Research in Veterinary Science*, *102*, 89–99. https://doi.org/10.1016/j.rvsc.2015.07.010

Mushahary, D., Spittler, A., Kasper, C., Weber, V., & Charwat, V. (2017). *Isolation , Cultivation , and Characterization of Human Mesenchymal Stem Cells*. https://doi.org/10.1002/cyto.a.23242

Nadia, N., Razali, M., Ng, C. T., Fong, L. Y., Sciences, H., Tunku, U., & Rahman, A. (2019). Cardiovascular Protective Effects of Centella asiatica and Its Triterpenes : A Review. *Planta medica, 85(16),* 1203–1215. https://doi.org/10.1055/a-1008-6138

Neurodegenerative Diseases. Retrieved January 23, 2022 from National Institute of Environmental Health Sciences website: https://www.niehs.nih.gov/research/supported/health/neurodegenerative/index.cfm#:~:text=Neurodegenerative%20diseases%20affect%20millions%20of%20people%20worldwide.%20Alzheimer%E2%80%99s

Nordin, N. (2021, December 16-19). *Neuroregenerative Properties of Centella asiatica on Oxidative Stress-Induced Stem Cell-derived Neural Cells* [Paper Presentation]. Indian Academy of Neurosciences (IAN) Society Meeting, India.

Ota, K. I. (2008). Fuel Cells: Past, Present and Future. *IEEJ Transactions on Fundamentals and Materials*, *128*(5), 329–332. https://doi.org/10.1541/ieejfms.128.329

Park, D., Xiang, A. P., Mao, F. F., Zhang, L., Di, C. G., Liu, X. M., Shao, Y., Ma, B. F., Lee, J. H., Ha, K. S., Walton, N., & Lahn, B. T. (2010). Nestin is required for the proper self-renewal of neural stem cells. *Stem Cells*, *28*(12), 2162–2171. https://doi.org/10.1002/stem.541

Pozzobon, M., Ghionzoli, Æ. M., Es, Á., Afs, Á. Á., & Surgery, Á. P. (2010). *ES , iPS , MSC , and AFS cells . Stem cells exploitation for Pediatric Surgery : current research and perspective*. 3–10. https://doi.org/10.1007/s00383-009-2478-8

Reza, S., Rostamabadi, H., Assadpour, E., & Jafari, S. M. (2020). *Morphology and microstructural analysis of bioactive-loaded micro / nanocarriers via microscopy techniques ; CLSM / SEM / TEM / AFM*. *280*. https://doi.org/10.1016/j.cis.2020.102166

Sears, V., & Ghosh, G. (2011). 乳鼠心肌提取 HHS Public Access. *Physiology & Behavior*, *176*(5), 139–148. https://doi.org/10.1002/bit.27272.Harnessing

Seyfizadeh, N., Seyfizadeh, N., Rahbarghazi, R., Nourazarian, A., Borzouisileh, S., Palideh, A., Elahimanesh, F., Hamishehkar, H., Salimi, L., Nouri, M., & Abtin, M. (2019). Isolation and characterization of human amniotic fluid and SH-SY5Y/BE(2)-M17 cell derived exosomes. *Acta Neurobiologiae Experimentalis*, *79*(3), 261–269. https://doi.org/10.21307/ane-2019-024

Shang, Z., Chen, D., Wang, Q., Wang, S., Deng, Q., Wu, L., Liu, C., Ding, X., Wang, S., Zhong, J., Zhang, D., Cai, X., Zhu, S., Yang, H., Liu, L., Fink, J. L., Chen, F., Liu, X., Gao, Z., & Xu, X. (2018). Single-cell RNA-seq reveals dynamic transcriptome profiling in human early neural differentiation. *GigaScience*, *7*(11), 1–19. https://doi.org/10.1093/gigascience/giy117

Soares, R., Ribeiro, F. F., Lourenço, D. M., Rodrigues, R. S., Moreira, J. B., Sebastião, A. M., Morais, V. A., & Xapelli, S. (2021). The neurosphere assay : an effective in vitro technique to study neural stem cells. *Neural regeneration research, 16(11), 2229–2231*. https://doi.org/10.4103/1673-5374.310678

Soumyanath, A., Zhong, Y., Gold, S. A., Yu, X., Koop, D. R., Bourdette, D., & Gold, B. G. (2005). *Centella asiatica accelerates nerve regeneration upon oral administration and contains multiple active fractions increasing neurite elongation in-vitro*. 1221–1229. https://doi.org/10.1211/jpp.57.9.0018

Théry, C., Witwer, K. W., Aikawa, E., Alcaraz, M. J., Anderson, J. D., Andriantsitohaina, R., Antoniou, A., Arab, T., Archer, F., Atkin-smith, G. K., Ayre, D. C., Bach, J., Bachurski, D., Baharvand, H., Balaj, L., Baldacchino, S., Bauer, N. N., Baxter, A. A., Bebawy, M., … Chen, C. (2018). *Minimal information for studies of extracellular vesicles 2018 (MISEV2018): a position statement of the International Society for Extracellular Vesicles and update of the MISEV2014 guidelines*. *7*. https://doi.org/10.1080/20013078.2018.1535750

Théry, C., Zitvogel, L., Amigorena, S., & Roussy, I. G. (2002). *EXOSOMES : COMPOSITION , BIOGENESIS AND FUNCTION*. *2*(August). https://doi.org/10.1038/nri855

Timmers, L., Lim, S. K., Arslan, F., Armstrong, J. S., Hoefer, I. E., Doevendans, P. A., Piek, J. J., El Oakley, R. M., Choo, A., Lee, C. N., Pasterkamp, G., & de Kleijn, D. P. V. (2008). Reduction of myocardial infarct size by human mesenchymal stem cell conditioned medium. *Stem Cell Research*, *1*(2), 129–137. https://doi.org/10.1016/j.scr.2008.02.002

Tögel, F., Hu, Z., Weiss, K., Isaac, J., Lange, C., & Westenfelder, C. (2005). Administered mesenchymal stem cells protect against ischemic acute renal failure through differentiation-independent mechanisms. *American Journal of Physiology - Renal Physiology*, *289*(1 58-1), 31–42. https://doi.org/10.1152/ajprenal.00007.2005

Ullah, M. O., Sultana, S., Haque, A., & Tasmin, S. (2009). Antimicrobial, cytotoxic and antioxidant activity of Centella asiatica. *Eur J Sci Res*, *30*(2), 260-264.

Walentowicz, P., Sadlecki, P., Bajek, A., Grabiec, M., & Drewa, T. (2022). Human amniotic fluid as a source of stem cells. *Open medicine (Warsaw, Poland), 17(1), 648–660*. https://doi.org/10.1515/med-2022-0468

Welbat, J. U., Chaisawang, P., & Pannangrong, W. (2018). *Neuroprotective Properties of Asiatic Acid against 5-Fluorouracil Chemotherapy in the Hippocampus in an Adult Rat Model*. https://doi.org/10.3390/nu10081053

Wong, J. H., Muthuraju, S., Reza, F., Senik, M. H., Zhang, J., Mohd Yusuf Yeo, N. A. B., Chuang, H. G., Jaafar, H., Yusof, S. R., Mohamad, H., Tengku Muhammad, T. S., Ismail, N. H., Husin, S. S., & Abdullah, J. M. (2019). Differential expression of entorhinal cortex and hippocampal subfields α-amino-3-hydroxy-5-methyl-4-isoxazolepropionic acid (AMPA) and N-methyl-D-aspartate (NMDA) receptors enhanced learning and memory of rats following

administration of Centella asiatica. *Biomedicine and Pharmacotherapy*, *110*(November 2018), 168–180. https://doi.org/10.1016/j.biopha.2018.11.044

Yogeswaran, L., Norazzila, O., & A, N. N. (2016). Recent Updates in Neuroprotective and Neuroregenerative Potential of Centella asiatica. *The Malaysian journal of medical sciences : MJMS, 23(1),* 4–14.

Zabeo, D., Cvjetkovic, A., Lässer, C., Schorb, M., Lötvall, J., & Höög, J. L. (2017). Exosomes purified from a single cell type have diverse morphology. *Journal of Extracellular Vesicles*, *6*(1). https://doi.org/10.1080/20013078.2017.1329476

Zaher, W., Harkness, L., & Jafari, A. (2014). *An update of human mesenchymal stem cell biology and their clinical uses*. 1069–1082. https://doi.org/10.1007/s00204-014-1232-8

Zhang, Y., Bi, J., Huang, J., Tang, Y., Du, S., & Li, P. (2020). Exosome : A Review of Its Classification , Isolation Techniques , Storage , Diagnostic and Targeted Therapy Applications. *International journal of nanomedicine*, *15*, *6917–6934*. https://doi.org/10.2147/IJN.S264498

APPENDICES

APPENDIX A

The average diameter of neurospheres.
Data are representative of P36 and P38 batches.

Group	**Average diameter of neurospheres,** μm **(Mean ± SD)**
Untreated	93.91 ± 27.19
1 μg/mL EECA	86.82 ± 6.31
10 μg/mL EECA	82.13 ± 21.67
50 μM dBcAMP	87.21 ± 15.42

The average percentage of 50-100 μm neurospheres.
Data are representative of P36 and P38 batches.

Group	**Average percentage of 50-100 μm neurospheres,% (Mean ± SD)**
Untreated	40.00 ± 56.57
1 μg/mL EECA	70.07 ± 24.66
10 μg/mL EECA	60.79 ± 8.32
50 μM dBcAMP	58.33 ± 35.36

The normalized corrected total cell fluorescence (CTCF) of nestin to DAPI.
Data are representative of P36 batch.

Group	Normalized CTCF of nestin to DAPI (Mean ± SD)
Untreated	2.85 ± 1.67
1 μg/mL EECA	3.12 ± 0.53
10 μg/mL EECA	N/A
50 μM dBcAMP	1.35 ± 0.00

The average diameter of exosomes.
Data are representative of P38 and P40 batches.

Group	Average diameter of exosomes, nm (Mean ± SD)
Untreated	79.30 ± 19.21
1 μg/mL EECA	79.49 ± 21.05
10 μg/mL EECA	114.8 ± 49.73
50 μM dBcAMP	70.82 ± 4.50

APPENDIX B

The average diameter of neurospheres.
Data are representative of P40 batch.

Group	**Average diameter of neurospheres,** μm **(Mean ± SD)**
Untreated	65.43 ± 17.53
1 μg/mL EECA	52.83 ± 11.61
10 μg/mL EECA	46.47 ± 12.15
50 μM dBcAMP	59.97 ± 15.27

The percentage of 50-100 μm neurospheres.
Data are representative of P40 batch.

Group	**Percentage of 50-100 μm neurospheres, %**
Untreated	71.43
1 μg/mL EECA	45.00
10 μg/mL EECA	36.11
50 μM dBcAMP	71.84